APEC Climate Symposium 2014
Nanjing, China

Asia-Pacific Economic Cooperation

HYDRO-METEOROLOGICAL VARIABILITY AND ITS INTEGRATED FLOOD RISK ASSESSMENT FOR THE KOREAN HAN RIVER BASIN DURING DIFFERENT EL NIÑO PHASES

(28. Oct. 2014)

Sun-kwon Yoon

APCC APEC CLIMATE CENTER

Contents

I Introduction

APCC
APEC CLIMATE CENTER

Research Goal

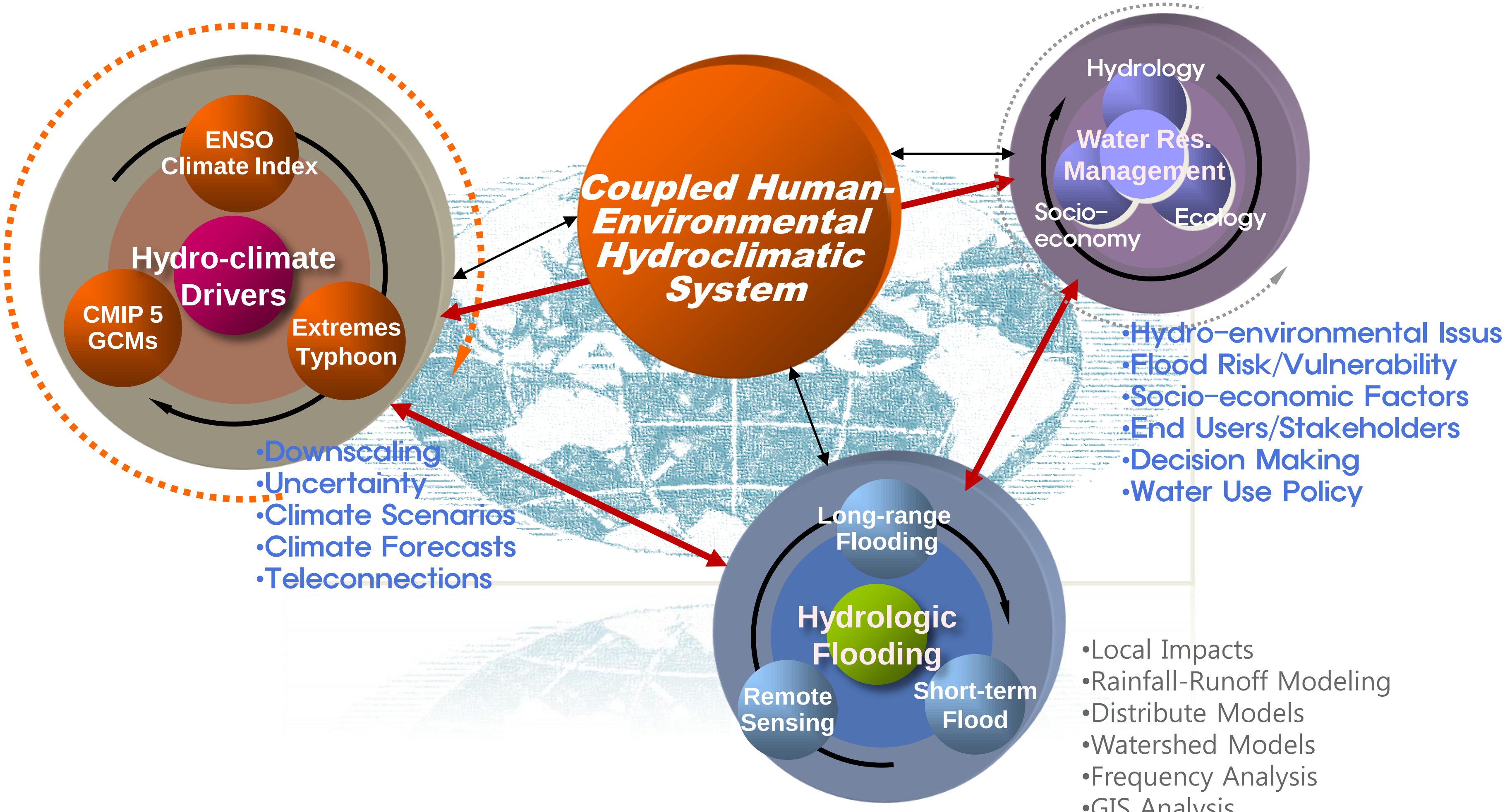

APCC APEC CLIMATE CENTER

Interdisciplinary work in APCC

By Coupling with Hydro-climate, Remote Sensing, and Advanced Hydrology for Extreme FLOOD and Heavy Rainfall analysis

A. *Extreme Climate Patterns and its Long-range Flood Forecasting*

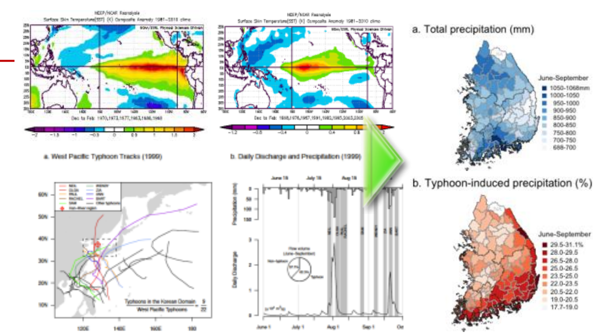

B. *Atmospheric Model-based Rainfall Forecast (RS, Radar, WRF)*

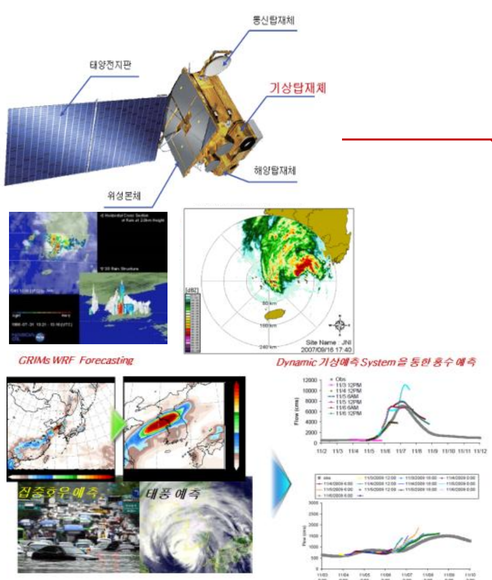

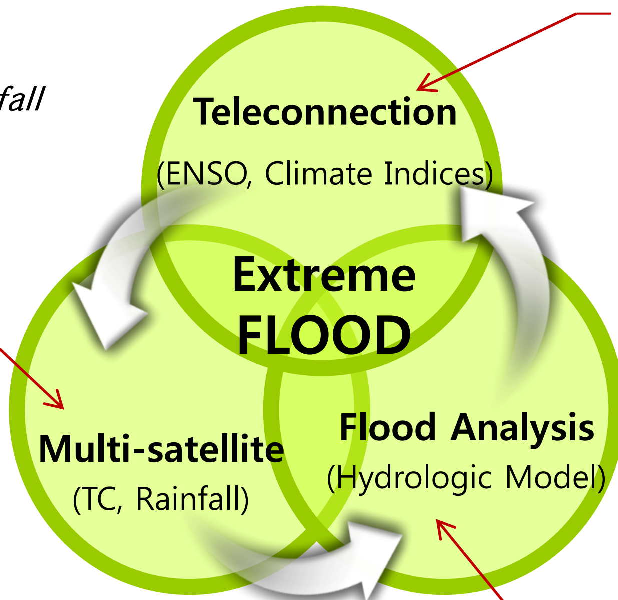

C. *Early Warning System for Flooding using R-Runoff Model Simulations*

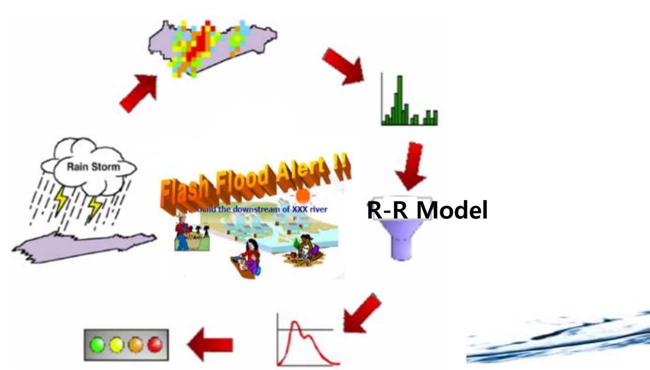

Background

- The **seasonal characteristics** of **hydrometeorological variability** are **closely related** to **global climate phenomena** and **climate changes** (*Wang et al. 2000; Grimm, 2011*).
- Investigating the significant correlation between **climatic factors** and **hydrologic data** is very important for the accurate **prediction and management of water resources** (*Horel and Wallace 1981; Pizarro and Lall 2002; Kim et al. 2011*).
- Moreover, **typhoons in the WNP** have a **strong influence on the hydrometeorological variables** over the Korean Peninsula (KP) during warm season. Recent climate have also indicated that the number and intensity of **TCs in the WNP are likely to increase slightly in the 21st century** (*Emanuel et al., 2008; Knutson et al., 2010*).
- In Korea, Nearly three-fourths of annual discharge occurs during the warm season (June–September). Warm season **hydroclimatology is a key determinant** of **extreme flood control** and **water resources management** in the KP.
- This research investigated the characteristic changes and physical mechanism in hydrologic variables that occur in the Korean major River Basin and their sub-watersheds in association with the **different ENSO phases** and **typhoon activities** in a changing climate.

Emerging Issues for Research

- New type of El Niño (Ashok and Yamagata, 2009)
- Projection of future typhoons (Knuston et al., 2010)

New type of El Niño

(Fig. 1a). But this might not be the only way of establishing morphogen gradients. In their studies of the morphogen Decapentaplegic (Dpp) protein in *Drosophila*, Kicheva *et al.*[3] photobleached a large region of the developing wing of the fly and measured the time it took for fluorescently labelled Dpp molecules to re-enter the bleached region. Their result — an effective diffusion coefficient of only ~0.1 μm²s⁻¹ — means that the typical time taken for Dpp to travel a certain distance would

CLIMATE CHANGE

The El Niño with a difference

Karumuri Ashok and Toshio Yamagata

Patterns of sea-surface warming and cooling in the tropical Pacific seem to be changing, as do the associated atmospheric effects. Increased global warming is implicated in these shifts in El Niño phenomena.

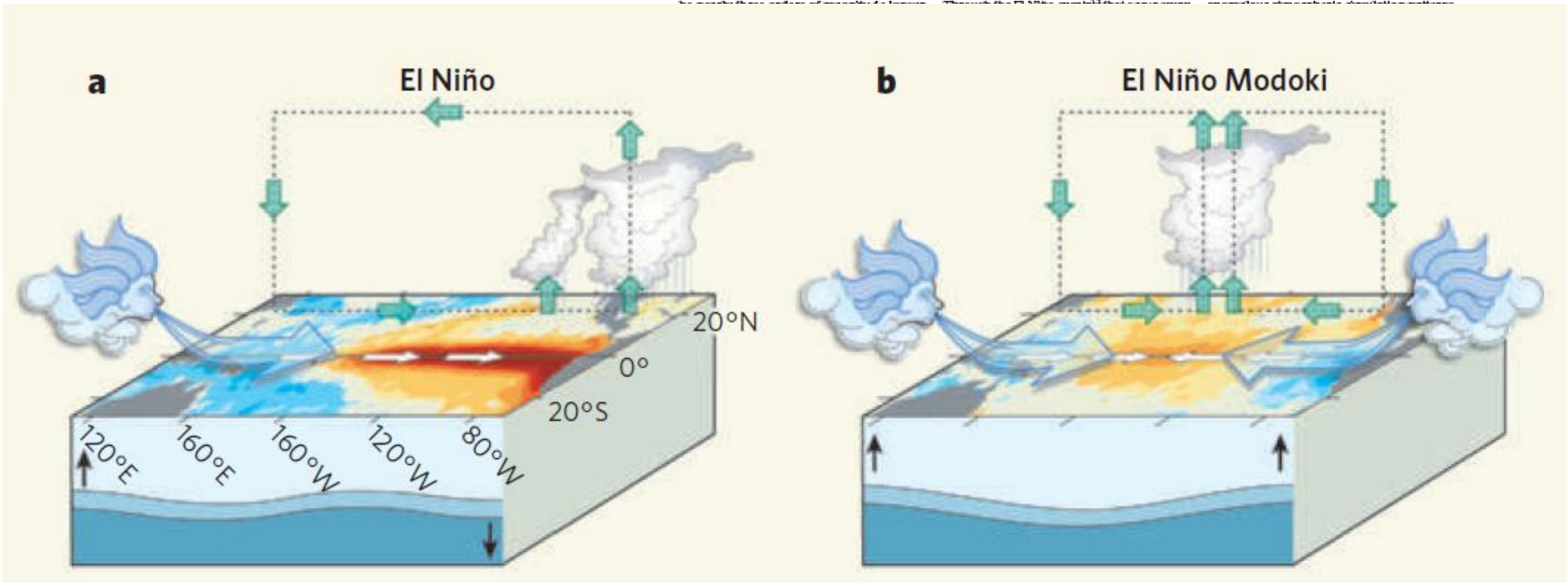

observed[8]. These are not like the conventional El Niño: rather, the maximum SST anomaly persists in the central Pacific from the boreal summer through to the winter, modifying the atmospheric circulation and resulting in distinctly different global impacts[4–11]. This phenomenon has been viewed as a different 'flavour' of El Niño[3], with warming around the Date Line rather than farther east[8]. In other studies[4,9,10] it has been classified as a new type of tropical Pacific phenomenon, and named

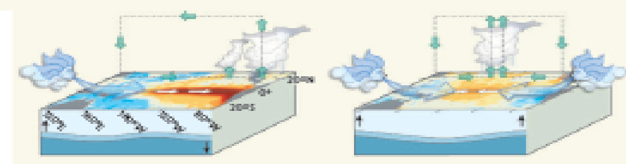

Modoki
: from the Japanese word meaning "similar, but different"

(Ashok and Yamagata, 2009)

Recent Researches

- Kao and Yu(2009), Contrasting eastern-Pacific and central-Pacific types of El Niño, *J. Climate*
- Kug et al(2009), Two types of El Niño events: Cold tongue El Niño and warm pool El Niño, *J.Climate*
- Yeh et al(2009), El Niño in a changing climate, *Nature*
- Feng et al(2011), Different impacts of El Niño and El Niño Modoki on China rainfall in the decaying phases, *IJOC*
- Na et al(2011), Statistical Simulations of the Future 50-year Satistics of Cold-Tongue El Niño and Warm-pool El Niño, *APJAS*
- Pradhan et al(2011), Modoki Indian Ocean Dipole and western North Pacific typhoons: Possible implications for extreme events, *JGR*
- Ren and Jin(2011), Niño indices for two types of ENSO, *GRL*
- Kug et al(2012), Improved simulation of two types of El Niño in CMIP5 models, *ERL*

- Sea Surface Temperatures (SST) in the tropical Pacific Ocean has been reported to have experienced a change in the cycle, intensity, and genesis of El Niño
- New type of El Niño phenomenon has caused changes in the hydrometeorological patterns throughout the world
- However, quantitative studies on features of CT/WP El Niño were found to be relatively insufficient for the Korean watersheds

Projections of future typhoons

nature geoscience
REVIEW ARTICLE
PUBLISHED ONLINE: 21 FEBRUARY 2010 | DOI: 10.1038/NGEO779

Tropical cyclones and climate change

Thomas R. Knutson[1]*, John L. McBride[2], Johnny Chan[3], Kerry Emanuel[4], Greg Holland[5], Chris Landsea[6], Isaac Held[1], James P. Kossin[7], A. K. Srivastava[8] and Masato Sugi[9]

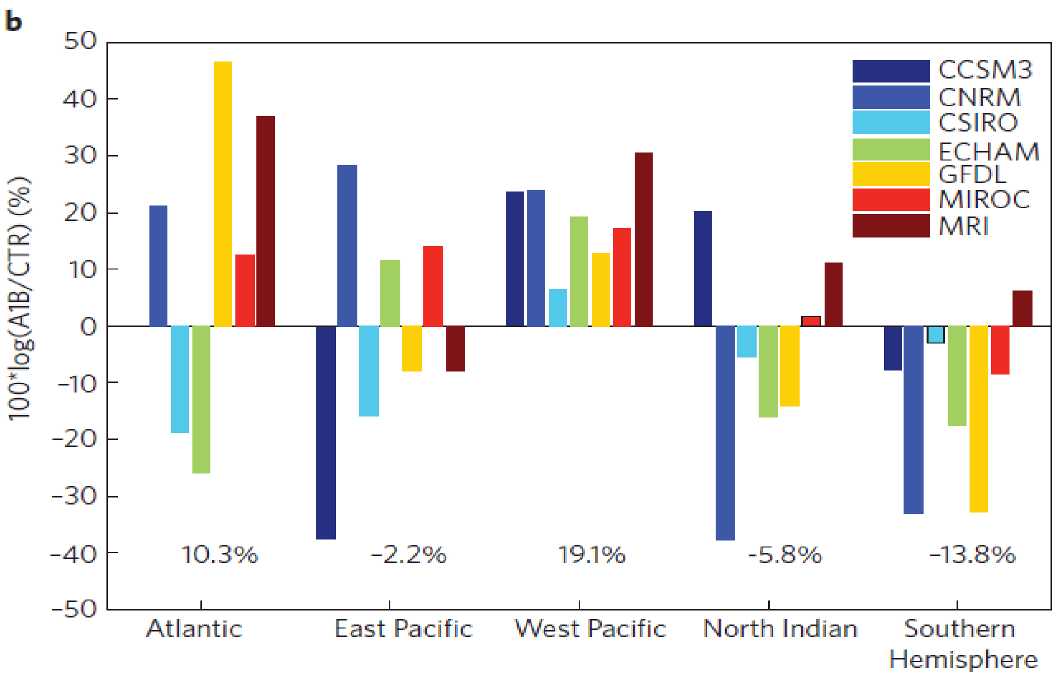

(Knutson et al., 2010)

Three research objectives

- To analyze the characteristics and sensitivity of hydrometeorological data during the warm season
- To analyze the effect of the different types of El Niño on rainfall and its Characteristic regional changes
- To provide basic information necessary for maintaining stable water supply and efficient management of water resources at the basin scale by analyzing the effect of CT/WP El Niño on TC-induced rainfall

❖ China's Flooding

- In 1887 flooding, 2 Million deaths (The Yellow River)
- In 1931 flooding, 4 Million deaths (The Yangtze River)
- In 1938 flooding, a Million deaths (The Yellow River)

--> China's Sorrow

❖ Thailand Flooding (Jul. – Sep., 2011)

Bangkok Flooding

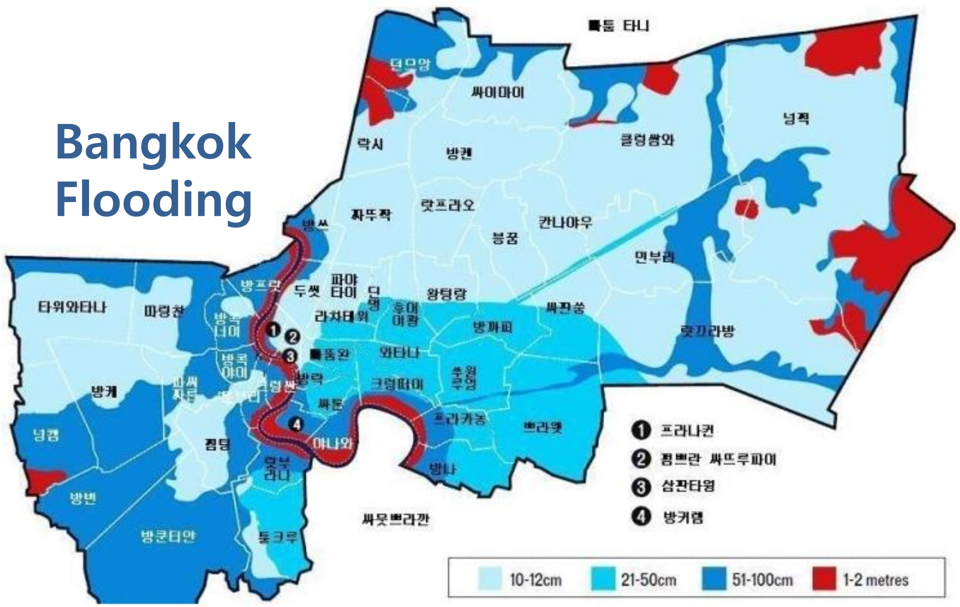

- Jul. 25- Sep., 2011, 3-month duration of Flooding
- One-third of the country, including also flooded Bangkok
- 283 lives death, 2Miliion affected, $0.51 Billion Damaged

India and Pakistan, Flooding (2010, 2014)

Deaths: 557 lives

Affected: 80,000 lives

Flooding: 2,500 villages

South Korea, Flooding (1990, 2002)

Han River
bank failure by Extreme Rainfall

Deaths : 163 lives
Affected : 187,265 lives
Damage : 52.03 Million dollars

Typhoon RUSA,
struck in Kangnung Province, South Korea

Deaths: 321 lives, Affected: 63,085 lives
Damage: 5.15 Billion dollars

II Analysis and Results

- Different Phases of ENSO and its Local Impacts
- Changes in Typhoon Activities over the KP
- Integrated Flood Risk Analysis in the Korean Han River Basin

APCC
APEC CLIMATE CENTER

(II-1) Different Phases of ENSO and its Local Impacts

Study Area

Figure 1. The 5 major river basin locations of Korean Peninsula (KP). Especially, the Han River Basin and its 24 sub-watersheds located in the center of the KP.

5 Major River Basin

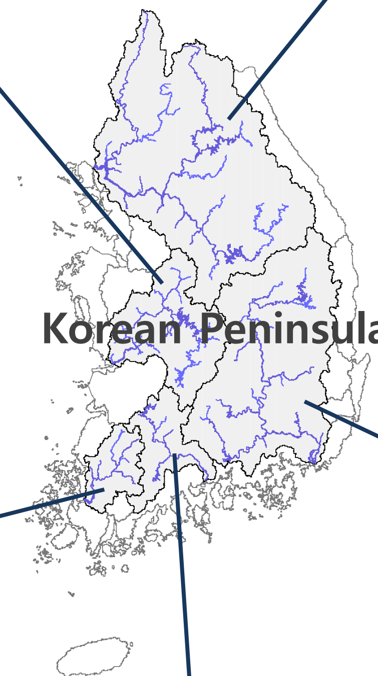

Keum River Basin

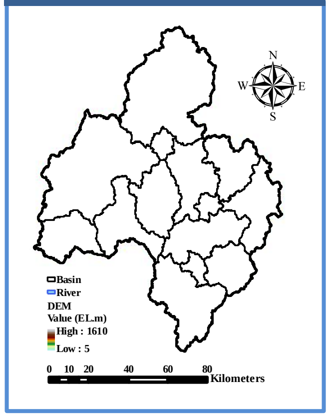

Han River Basin

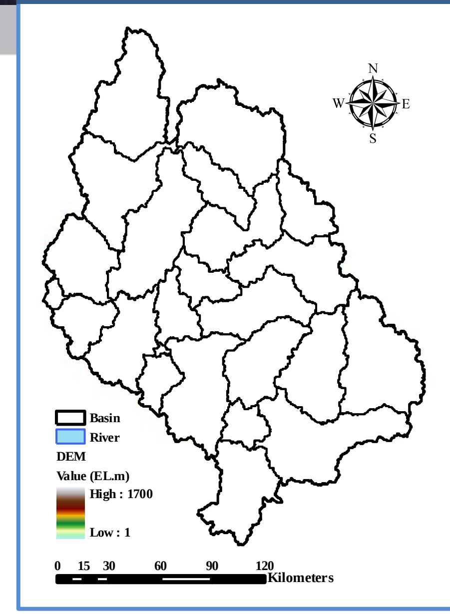

Youngsan River Basin

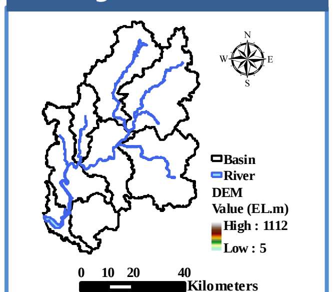

Seomjin River Basin

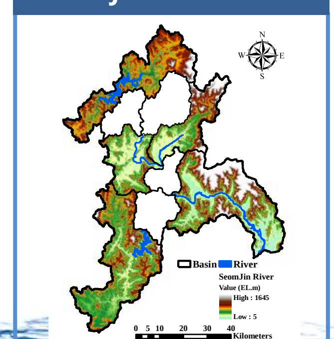

Nakdong River Basin

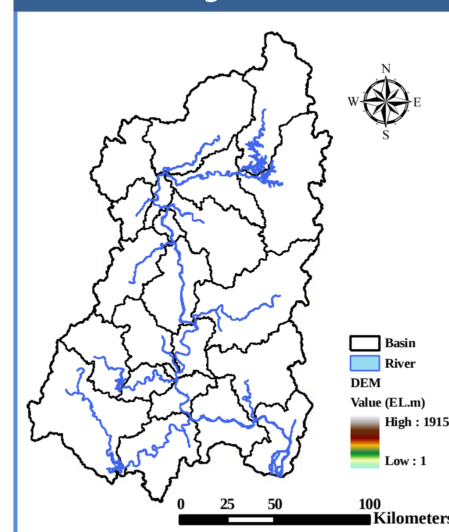

(a) Fractional Precipitation (Han River)

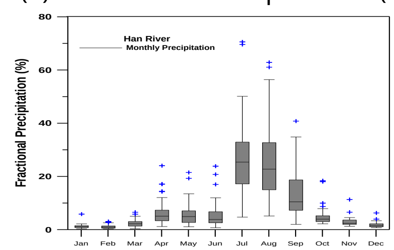

(b) Fractional Flow (Han River)

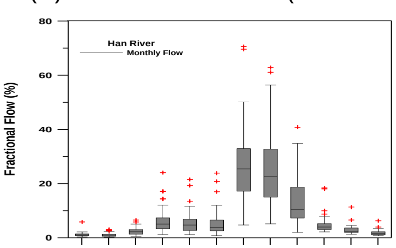

* Data From WAMIS (http://www.wamis.go.kr)

Two types of El Niño, SST Composite

- Different type of ENSO
  - CP/WP El Niño
  - El Niño Modoki

* CT/WP El Niño

$$N_{CT} = N_3 - \alpha N_4 \qquad \alpha = \begin{cases} 2/5, & N_3 N_4 > 0 \\ 0, & otherwise. \end{cases}$$

$$N_{WP} = N_4 - \alpha N_3$$

, by Ren and Jin (2011)

Figure 1. (a) Normalized Time series of N_3 (black) and N_{CT} (blue) indices, and (b) those of N_4 (black) and N_{WP} (pink) indices. Dotted grey lines indicate one standard deviation of N_{CT} and N_{WP} indices.

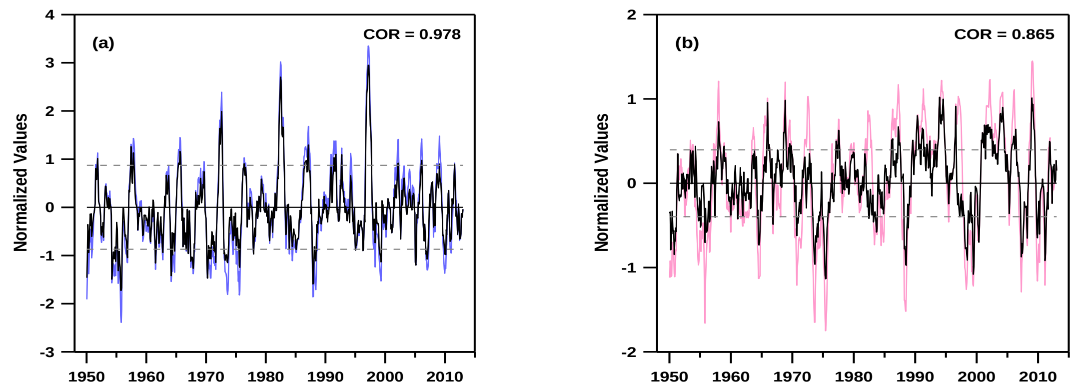

Figure 2. Scatter plots (a) for N_3 and N_4 indices, and (b) for N_{CT} and N_{WP} indices. CORs denote correlations between two indices in each panel.

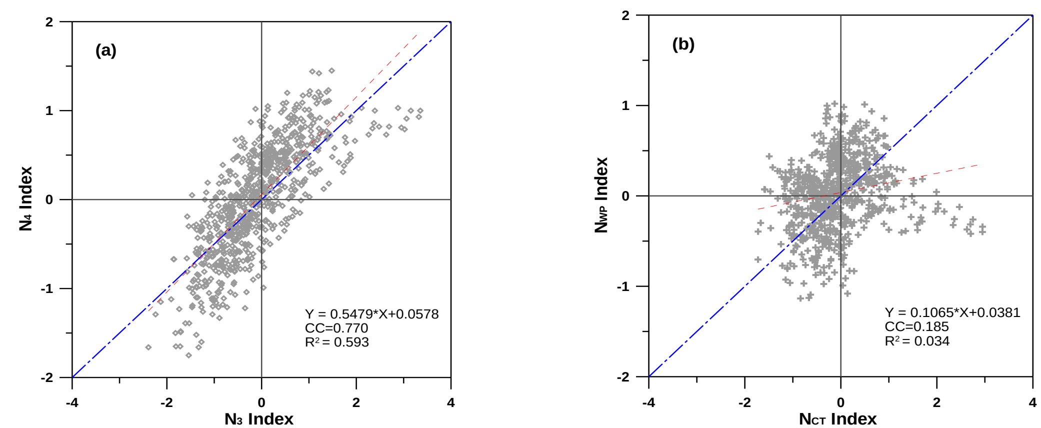

* Data From NOAA (http://www.esrl.noaa.gov/psd/cgi-bin/data/composites/printpage.pl)

Two types of El Niño Classification

Figure 3. Composite sea surface temperature anomalies (SSTA) in the developing phases of two types of El Niño during December-January.

(a) CT El Niño years (DJF)

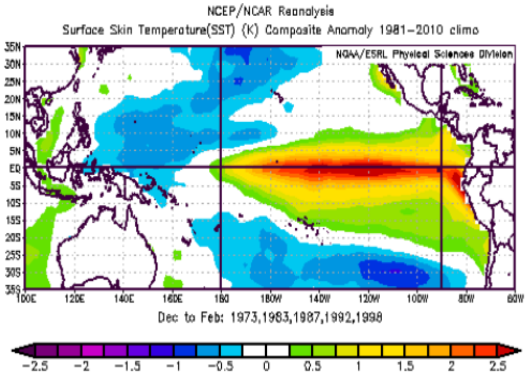

(b) WP El Niño years (DJF)

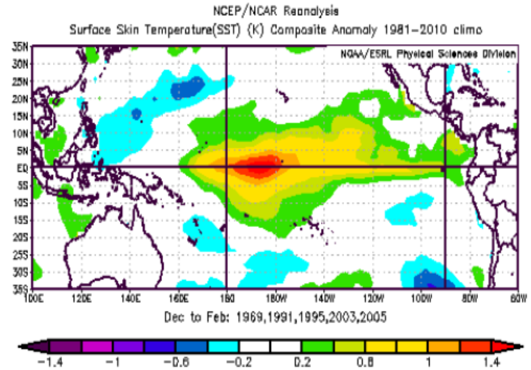

Table 4. Classification of the Strong CT El Niño years and Strong WP El Niño years.

El Niño Type	The Strong years during 1950-2011
CT El Niño	1972/73, 1982/83, 1986/87, 1991/92, 1997/98
WP El Niño	1968/69, 1990/91, 1994/95, 2002/03, 2004/05

- Source: ENSO data → (URL:http://www.cpc.ncep.noaa.gov/data/indices)

Global Precipitation Patterns over Asia

Figure 5. Composite anomalies of GPCP seasonal precipitation (MAM: March to May, JJA: June to August) during the CT El Niño and WP El Niño years over the Asia domain.

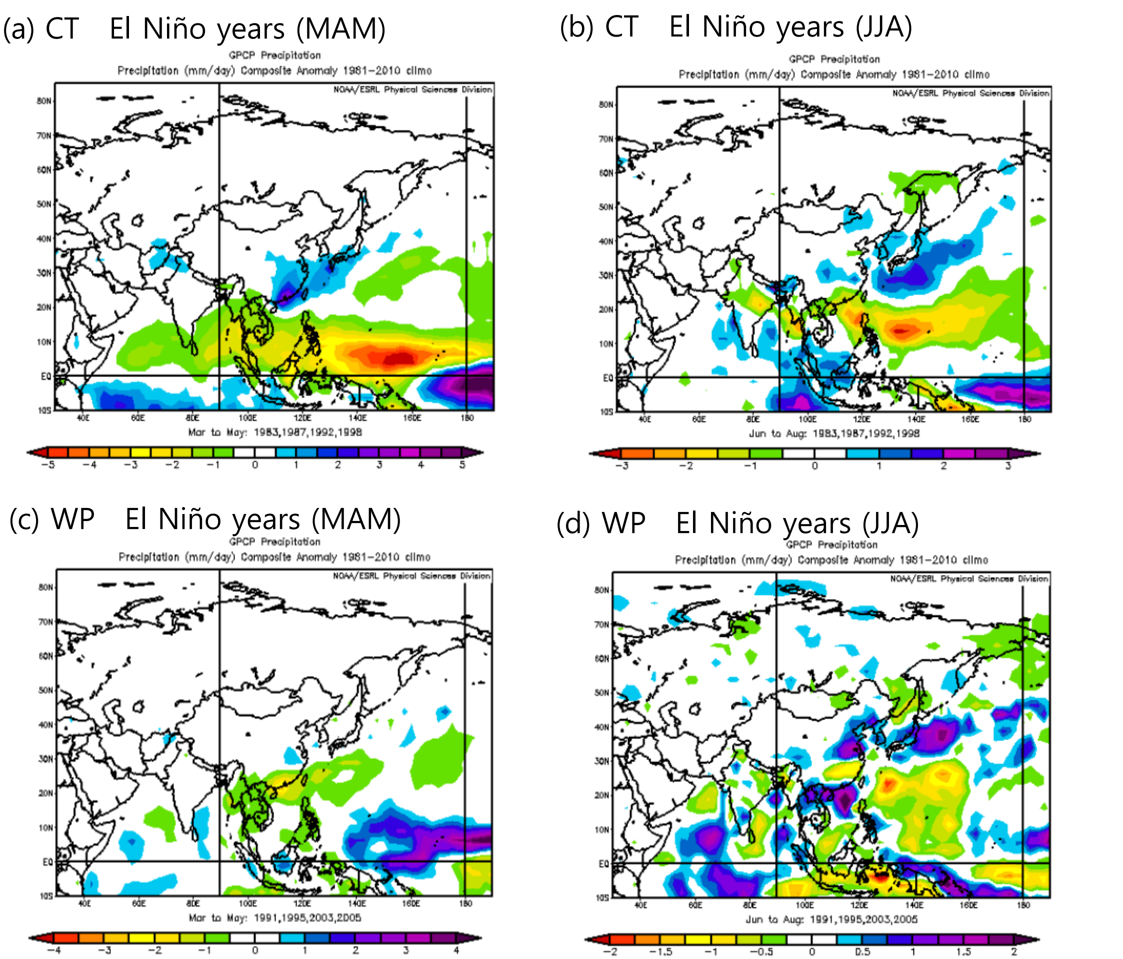

* Data From NOAA GPCP (global precipitation climatology project, http://www.esrl.noaa.gov/psd/cgi-bin/data/composites/printpage.pl)

Regional Precipitation Patterns over East Asia

Figure 6. Composite anomalies of GPCC precipitation and V6 combined seasonal (MAM: March to May, JJA: June to August) precipitation data during the CT El Niño and WP El Niño years.

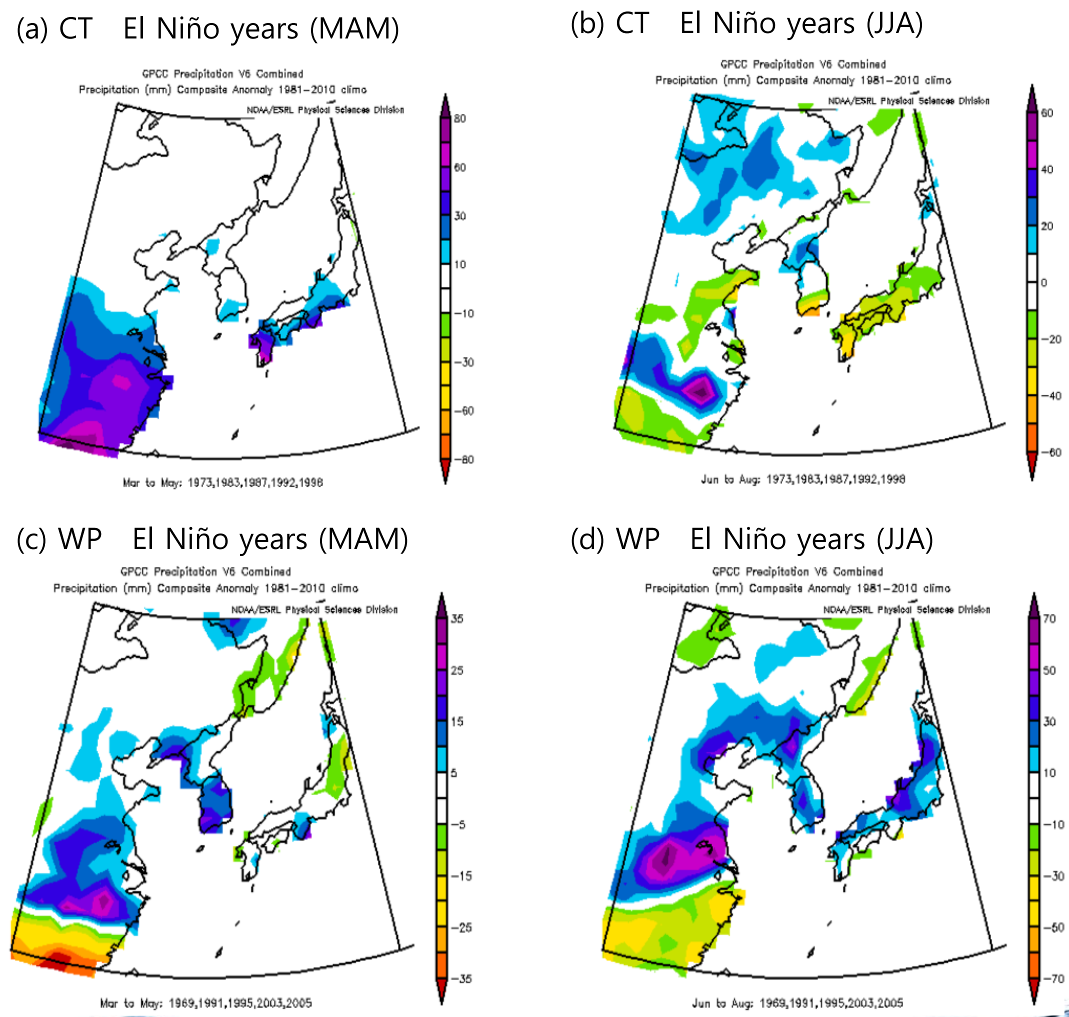

* Data From NOAA, (http://www.esrl.noaa.gov/psd/cgi-bin/data/composites/printpage.pl)

Seasonality

Figure 7. Annual total precipitation and seasonal mean precipitation over the Mid-watershed in the Han River basin.

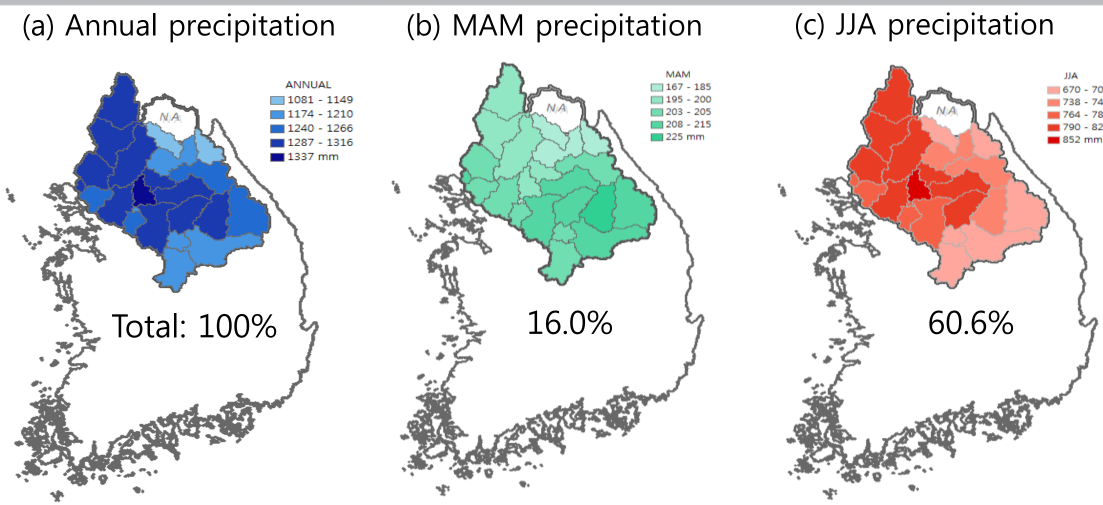

Figure 8. Percentage changes of seasonal fractional flows and the coefficient of variations during (a and c) spring season (March to May) and (b and d) summer season (June to August) over the Han River basin, Korea.

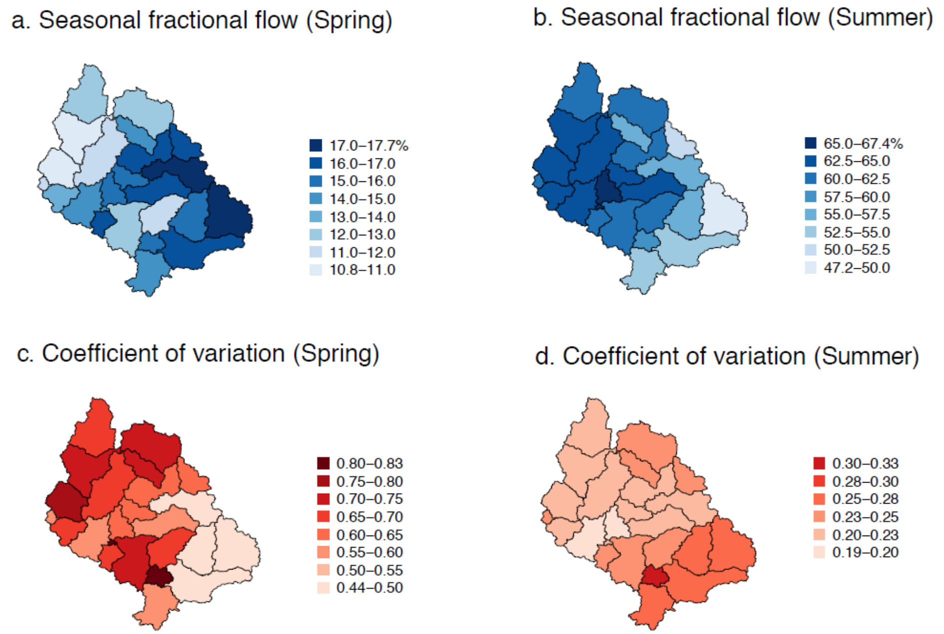

Empirical PDF using Kernel Density Function

*Kernel Estimate

$$\hat{f}_h(x) = n^{-1}\sum_{i=1}^{n} h^{-1} K\{h^{-1}(x-X_i)\}$$

*Bandwidth

$$h = \left[\frac{R(K)}{nR(\hat{f}''_{g(h)})\left(\int x^2K(x)dx\right)^2}\right]$$

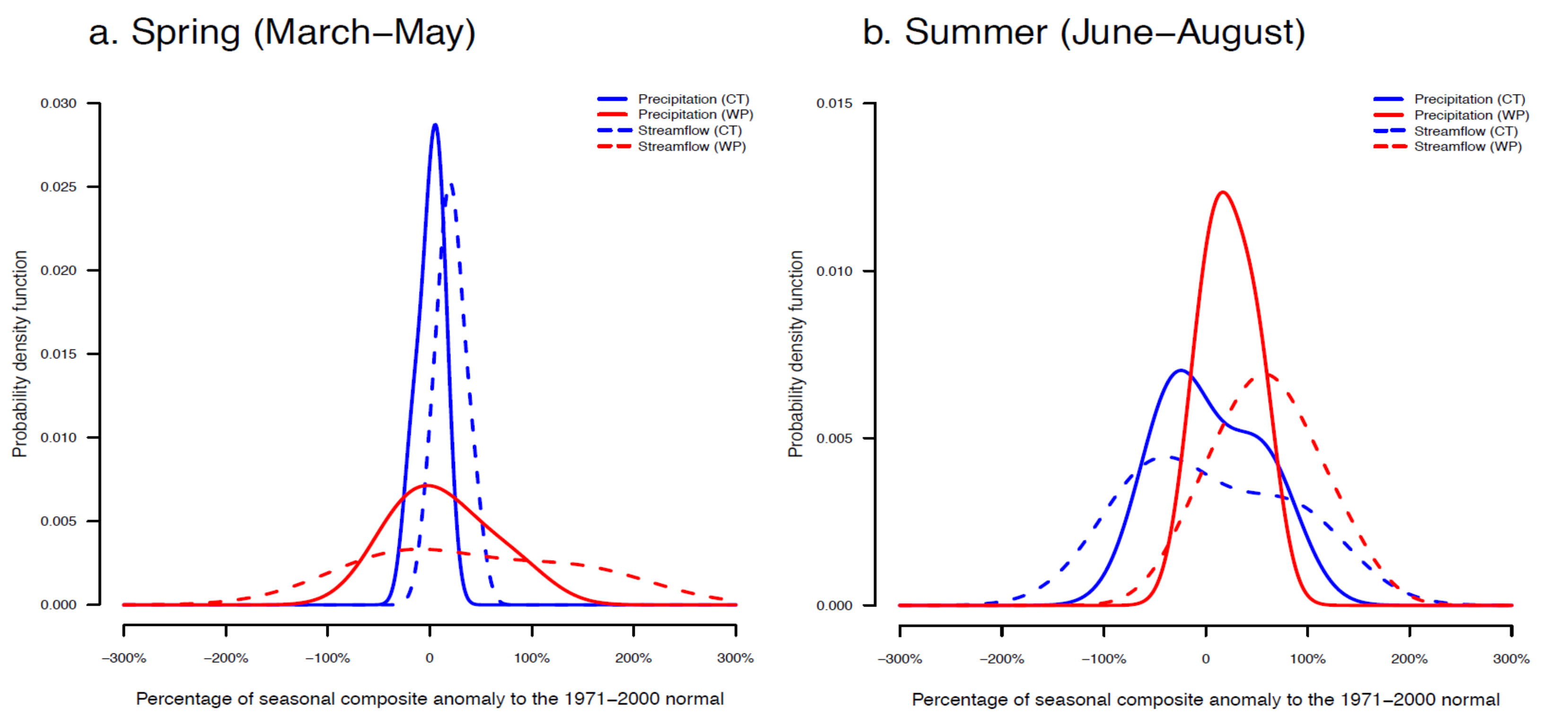

Figure 9. Empirical probability density function for the seasonal precipitation and the seasonal streamflow by percentage of seasonal composite anomalies during CT El Niño and WP El Niño over the spring and summer season over the Han River basin, Korea.

Hydrological Variability (MAM Precipitation)

Figure 10. Percentage changes of MAM precipitation and coefficient of variations in composite anomalies (departures from the 1971-2000 normals) during (a and c) CT El Niño years and (b and d) WP El Niño years over the Han River basin, Korea. The effects of both phases of ENSO are shown with different color schemes (increases in blues and decreases in reds). The hatched polygon shows statistically significant in seasonal precipitation (March to May) based on a 90 % confidence level.

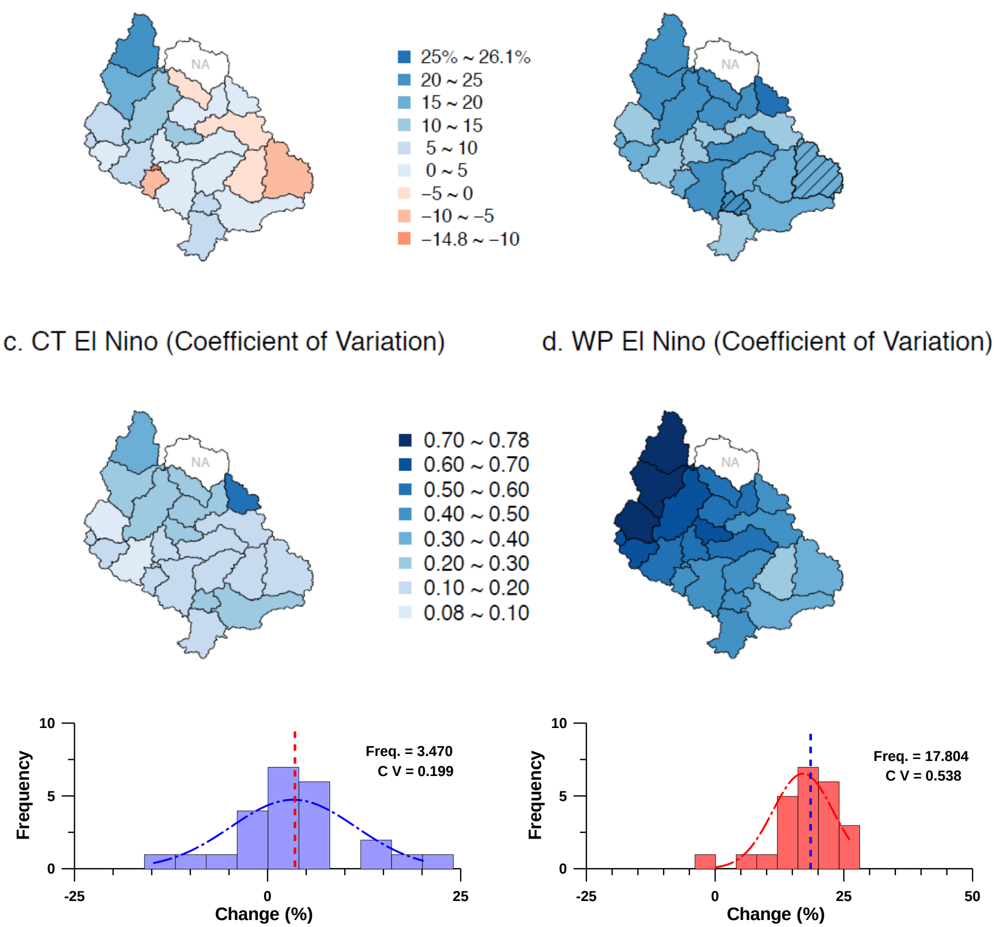

Hydrological Variability (JJA Precipitation)

Figure 11. Percentage changes of JJA precipitation and coefficient of variations in composite anomalies (departures from the 1971-2000 normals) during (a and c) CT El Niño years and (b and d) WP El Niño years over the Han River basin, Korea. The effects of both phases of ENSO are shown with different color schemes (increases in blues and decreases in reds). The hatched polygon shows statistically significant in seasonal precipitation (June to August) based on a 90 % confidence level.

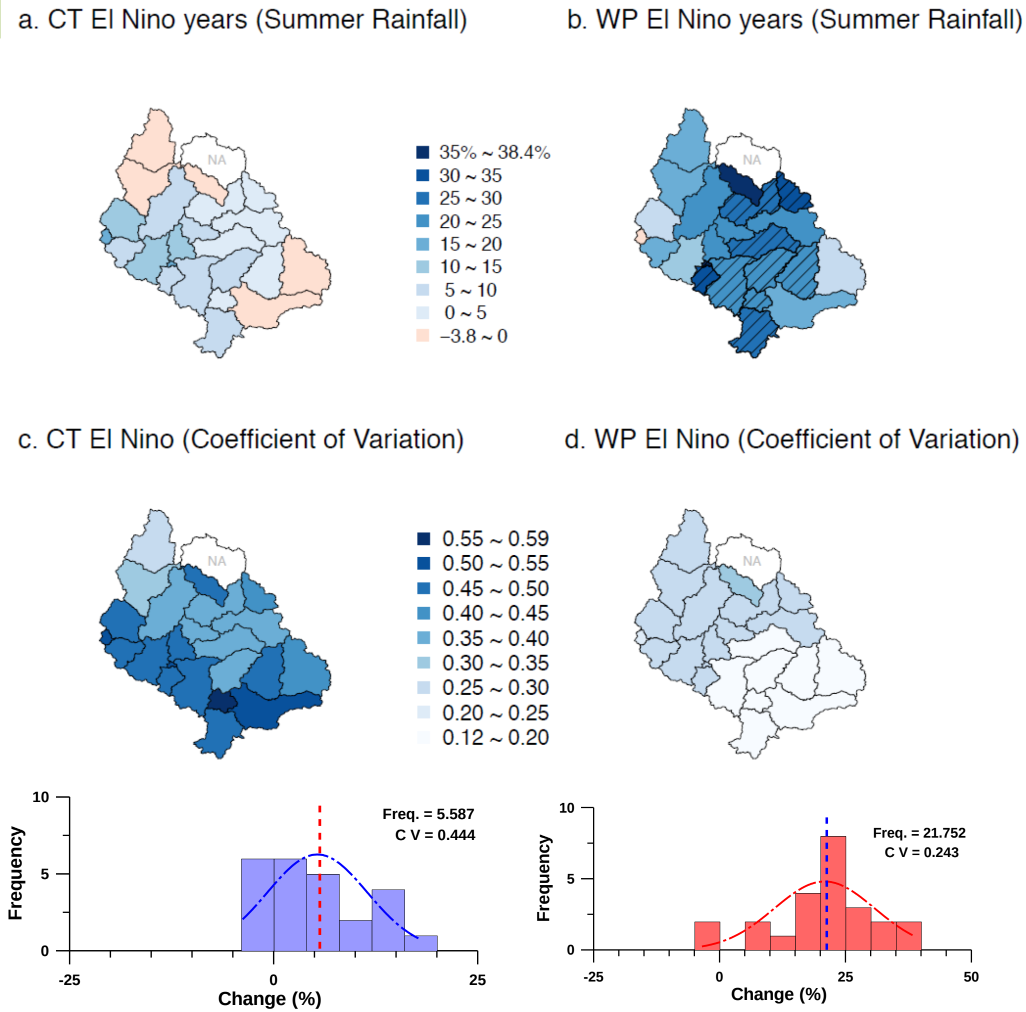

Hydrological Variability (MAM Streamflow)

Figure 12. Percentage changes and coefficient of variations in composite anomalies for MAM streamflow (departures from the 1971-2000 normals) during (a and c) CT El Niño years and (b and d) WP El Niño years over the Han River basin, Korea. The effects of both phases of ENSO are shown with different color schemes (increases in blues and decreases in reds). The hatched polygon shows statistically significant in seasonal streamflow (March to May) based on a 90 % confidence level.

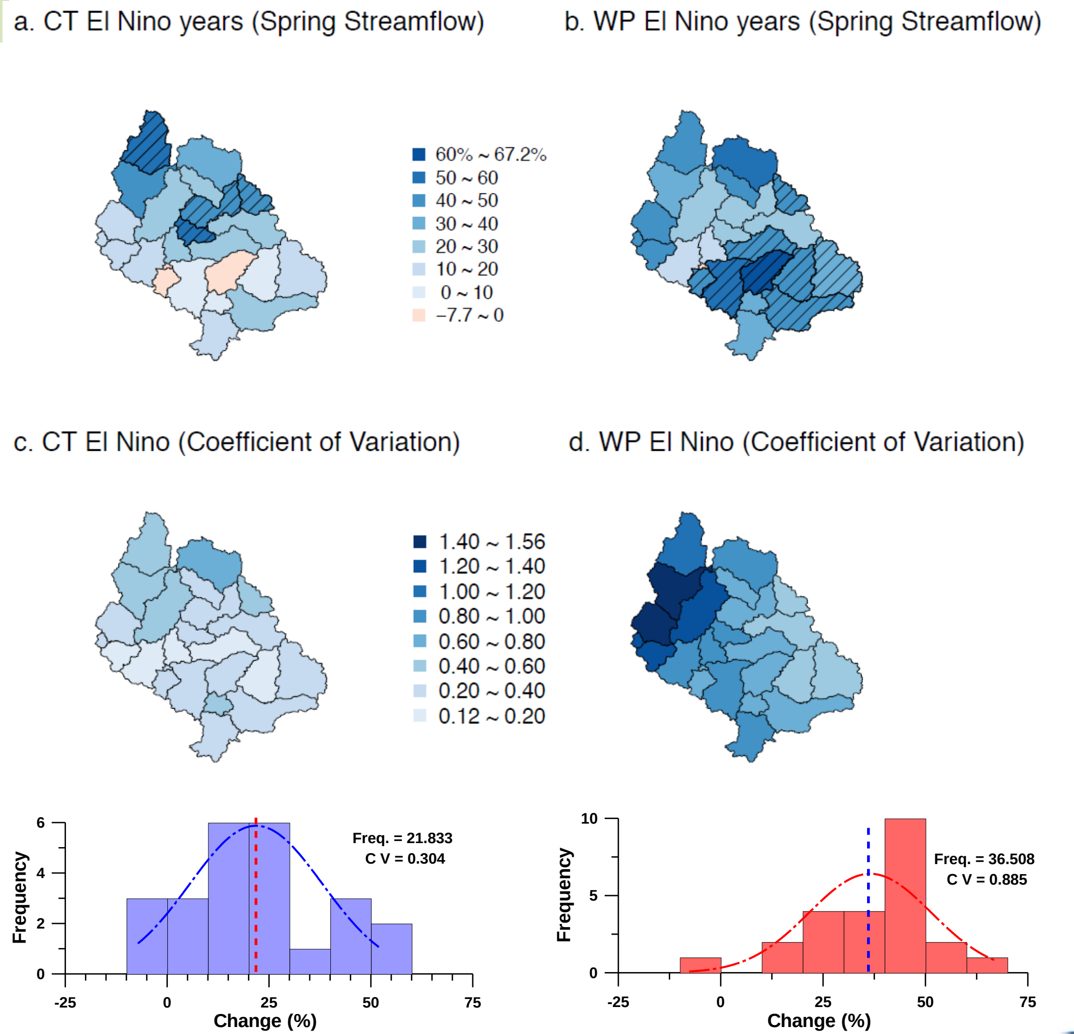

Hydrological Variability (JJA Streamflow)

Figure 13. Percentage changes and coefficient of variations in composite anomalies of JJA streamflow (departures from the 1971-2000 normals) during (a and c) CT El Niño years and (b and d) WP El Niño years over the Han River basin, Korea. The effects of both phases of ENSO are shown with different color schemes (increases in blues and decreases in reds). The hatched polygon shows statistically significant in seasonal streamflow (June to August) based on a 90 % confidence level.

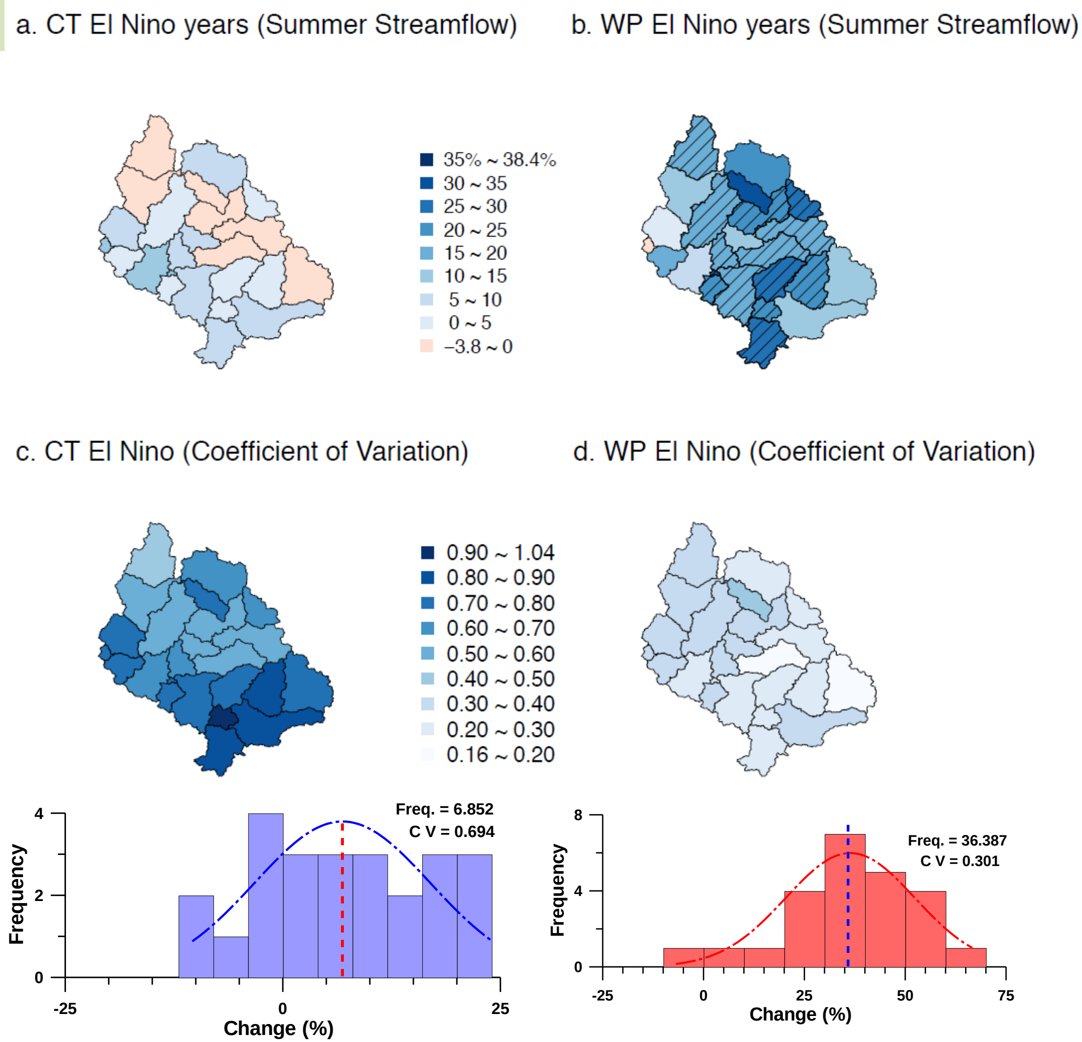

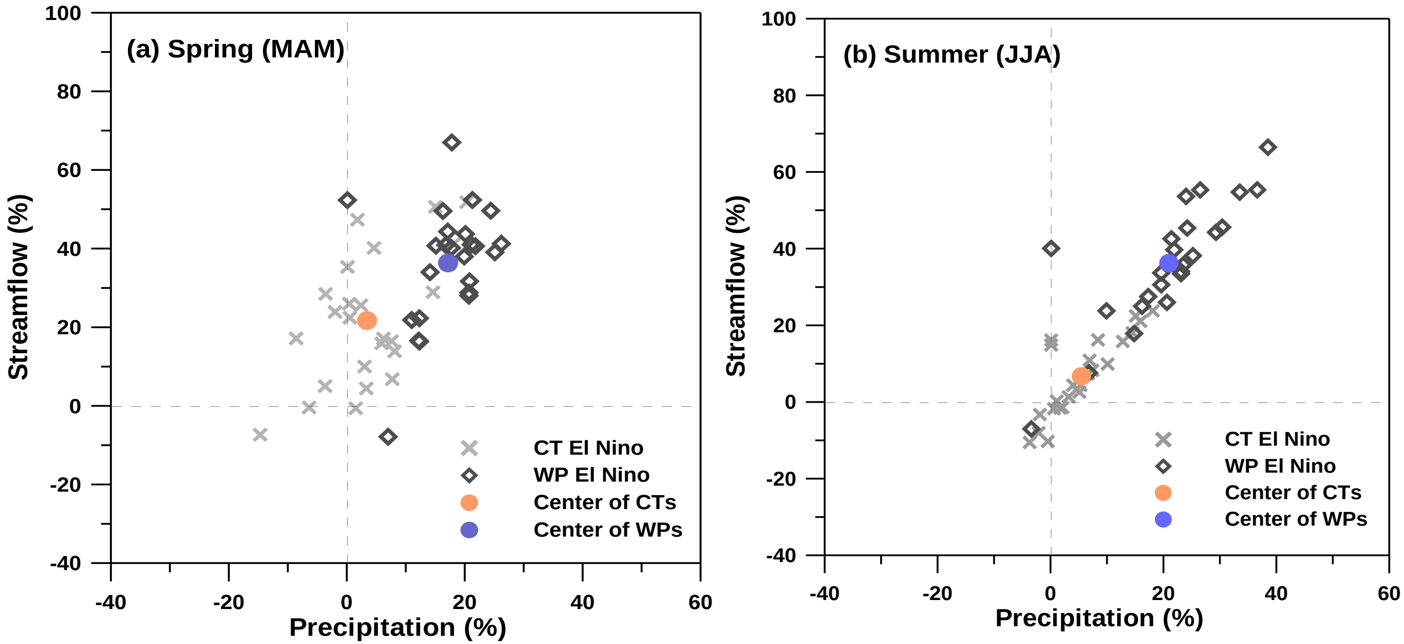

Figure 14. Percentage anomaly (departures from the 1971-2000 normals) changes between precipitation and streamflow in Spring (MAM) and Summer (JJA) season during different ENSO types over the Han River Basin and its sub-watersheds.

Table 3. Summary statistics in seasonal variability associated with different ENSO types

ENSO	Statistics	Spring (MAM)		Summer (JJA)	
		Precipitation	Streamflow	Precipitation	Streamflow
CT El Niño	Average Change (%)	3.47	5.59	21.83	6.85
	Significant (α=0.10)	NA	NA	4/23	NA
	CV	0.20	0.44	0.30	0.69
WP El Niño	Average Change (%)	17.80	21.75	36.51	36.39
	Significant (α=0.10)	2/23	10/23	8/23	14/23
	CV	0.54	0.24	0.89	0.30

APCC APEC CLIMATE CENTER

Hydrometeorological Variability over KP during JJAS Season

(a) WP El Nino (b) CT El Nino (c) La Nina

JJAS Precipitation

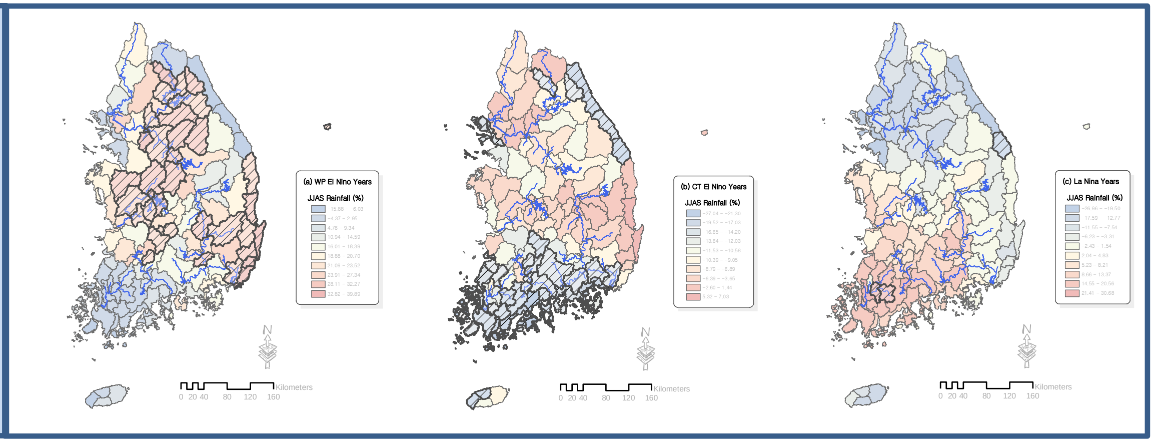

JJAS Streamflow

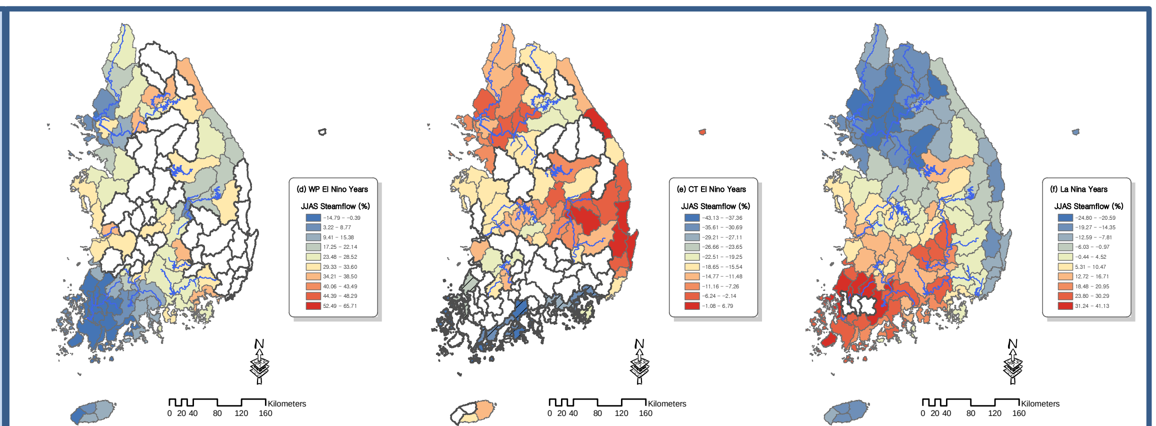

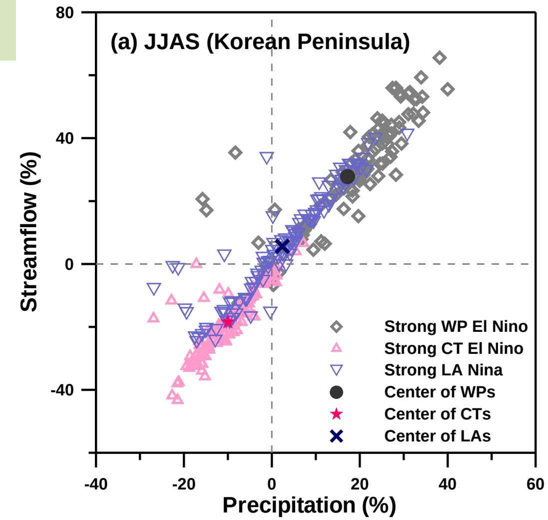

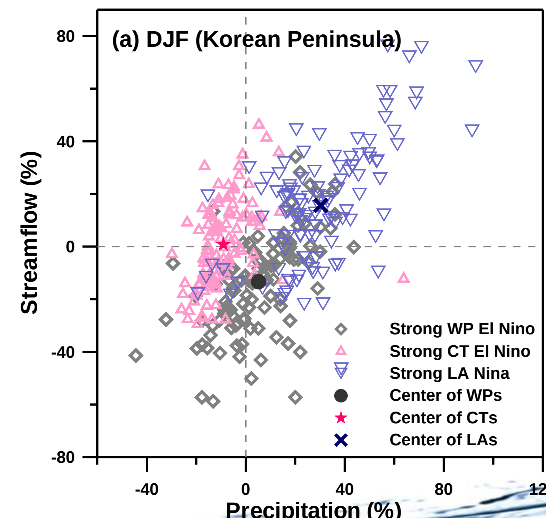

(II-2) Changes in Typhoon Activities over the Korean Peninsula

APCC APEC CLIMATE CENTER

Study Area

Figure 1. Distribution of seasonal precipitation (June–September) in Korea during the 1966–2007 periods. (a) Five major river basins in Korea. (b) Distribution of seasonal precipitation. The annual long-term average precipitation was noted with the number for each histogram. The fraction of seasonal precipitation and TC-induced precipitation are expressed in percentage.

a. Five major river basins in Korea

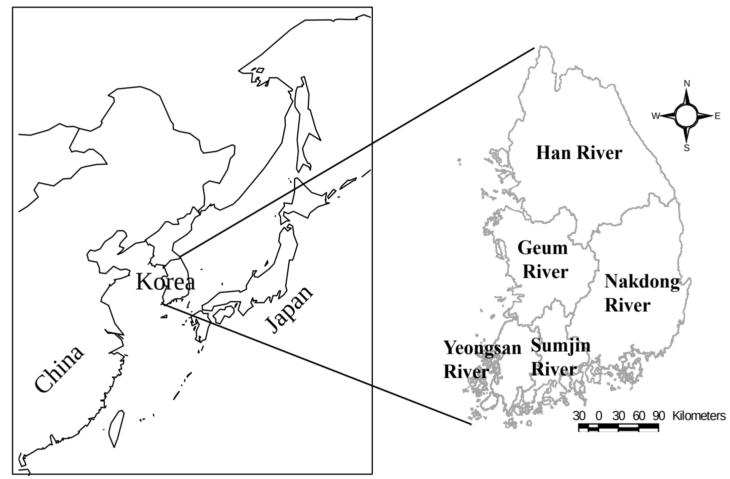

b. Distribution of seasonal precipitation

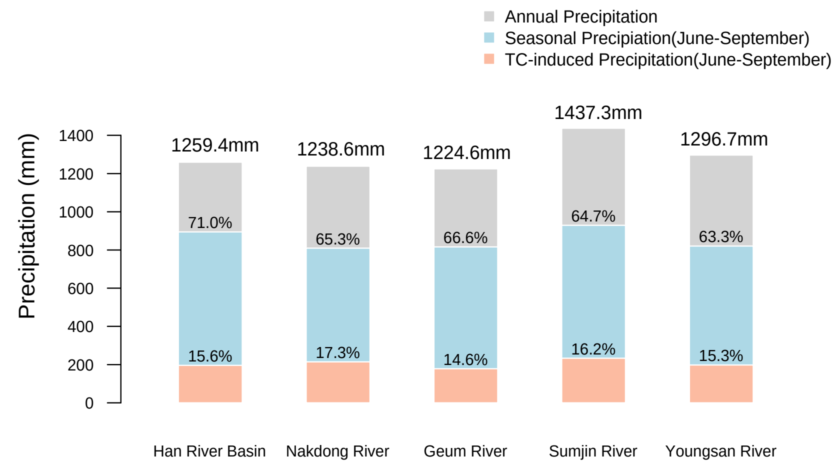

APCC APEC CLIMATE CENTER

TC Frequency / Intensity

Figure 2. TC frequency of the CT El Niño and WP El Niño years. The solid lines mean a climatological mean of TC frequency in each region (WNP: 16.13/year, KP: 5.0/year).

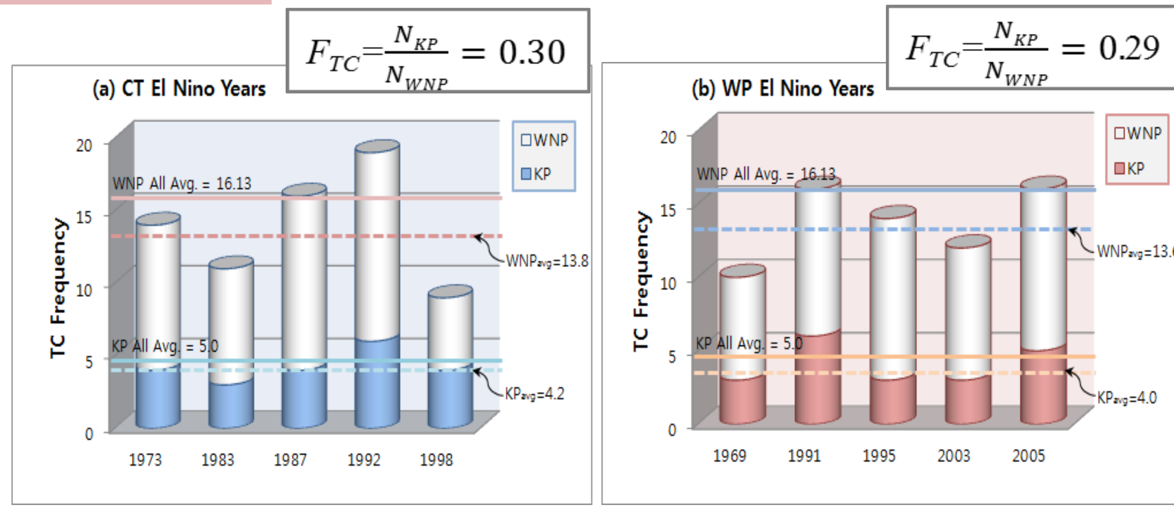

Figure 3. TC intensity of the CT El Niño and WP El Niño years. (a) means central pressure, and (b) means wind speed in each CT/WP El Niño year.

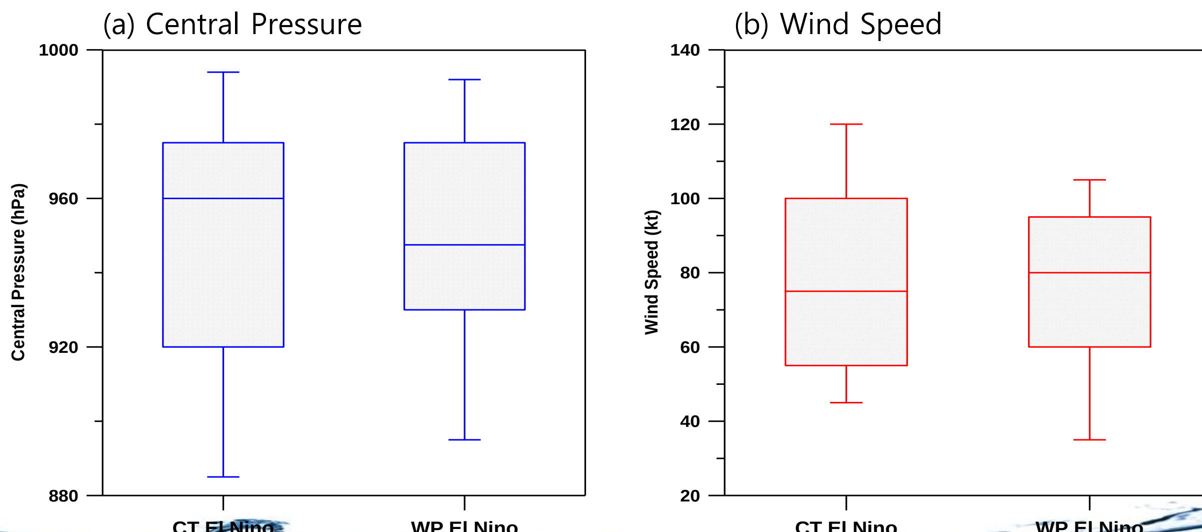

Large-Scale Environments

Figure 6. Composite differences of tropical cyclones (TCs) passed through the Korean domain (shown in a solid blue line) during CT and WP El Niño years. The solid (dashed) line indicates the seasonal mean (June-September) of the WNP subtropical high (5880 gpm) during the WP (CT) El Niño years.

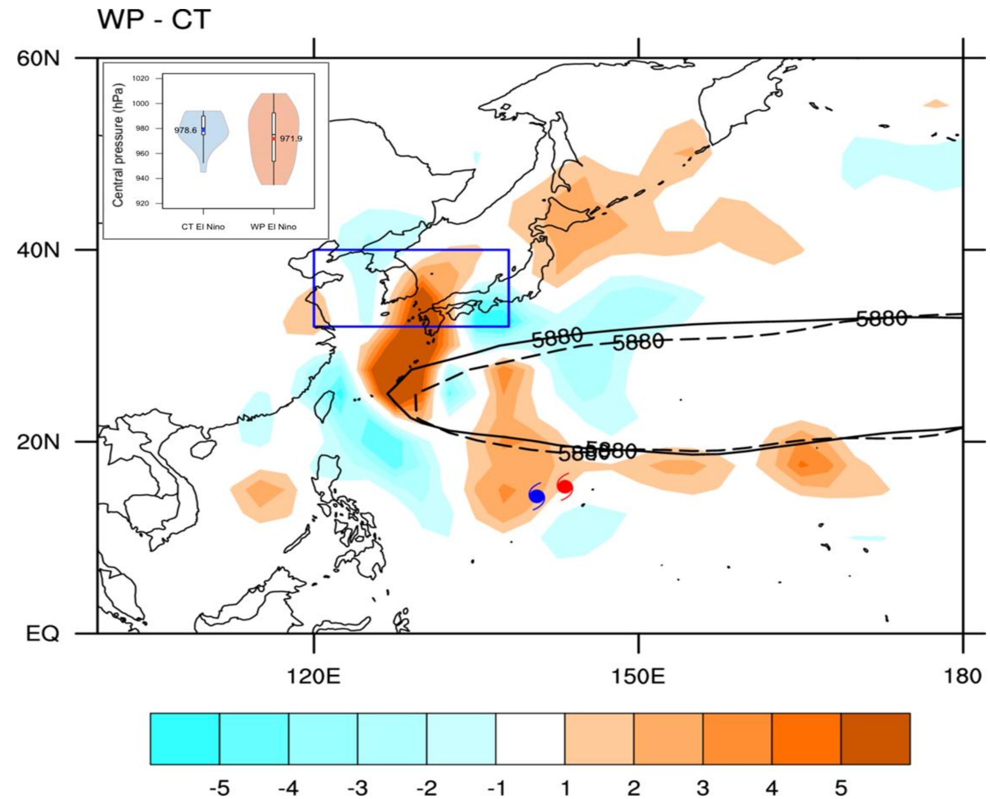

The movement route of typhoons frequently appeared to be widely spread and in an irregular zigzag pattern during CT El Niño years. During WP El Niño years, relatively powerful typhoons tended to move along the seas around the KP and along the Kuroshio.

Large-Scale Environments

Figure 7. SST-composed anomalies obtained from Hadley SST in (a) CT years and (b) WP years. Shading indicates values over 90% confidence based on Student's *t*-test.

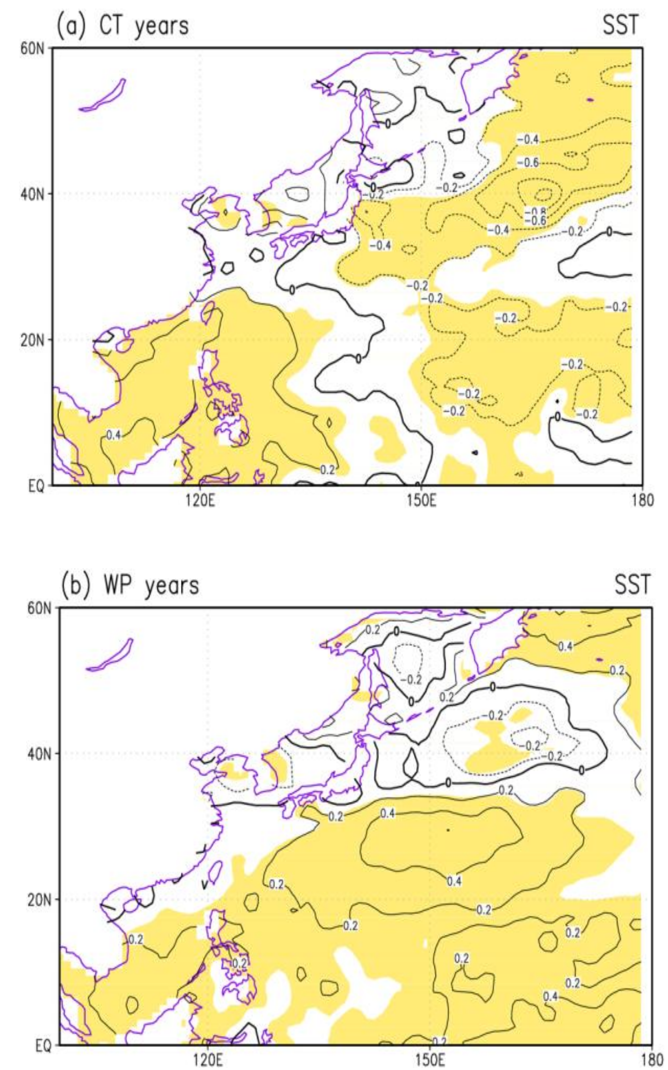

During WP El Niño years, SSTAs are comparatively high across the WNP, except for an extended area incorporating the eastern Kuroshio off Japan and the coastal seas off the KP. These higher SSTAs should provide favorable conditions for TC development as latent heat generation might reinforce or maintain the intensity of TCs that migrate northward towards the KP after forming at low latitudes

Large-Scale Environments

Figure 8. Vertical wind shear anomalies obtained from NCEP-NCAR reanalysis. Shading indicates values over 90% confidence based on Student's *t*-test.

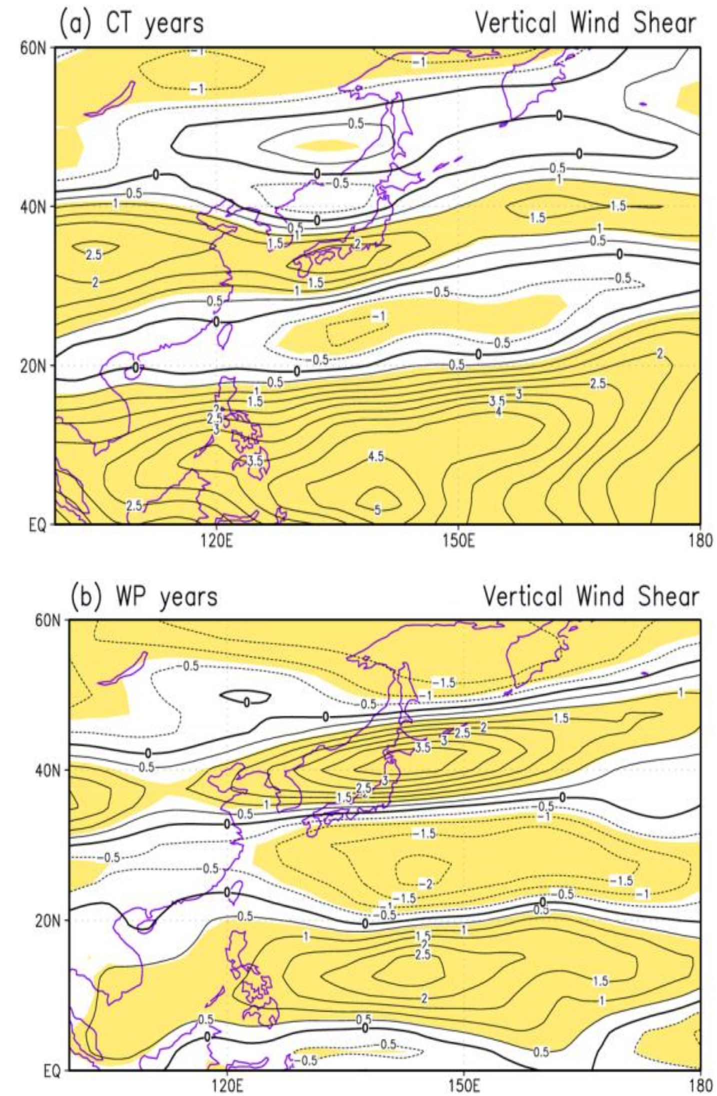

During the CT El Niño period, negative VWS anomalies appear to be narrow around latitude 20°, whereas a positive anomaly appears over latitude 25°. Meanwhile, during the WP El Niño period, negative VWS anomalies form a wider area from latitudes 20°N to 35°N. We assume that this negative VWS zone can maintain or reinforce the intensity of TCs that go north towards the KP

Local Impacts on TC-induced Heavy Rainfall

Figure 9. Composite anomalies of TC-induced rainfall during CT/WP El Niño years. The hatched polygons indicate statistically significant changes in TC rainfall based on the 10% significance level.

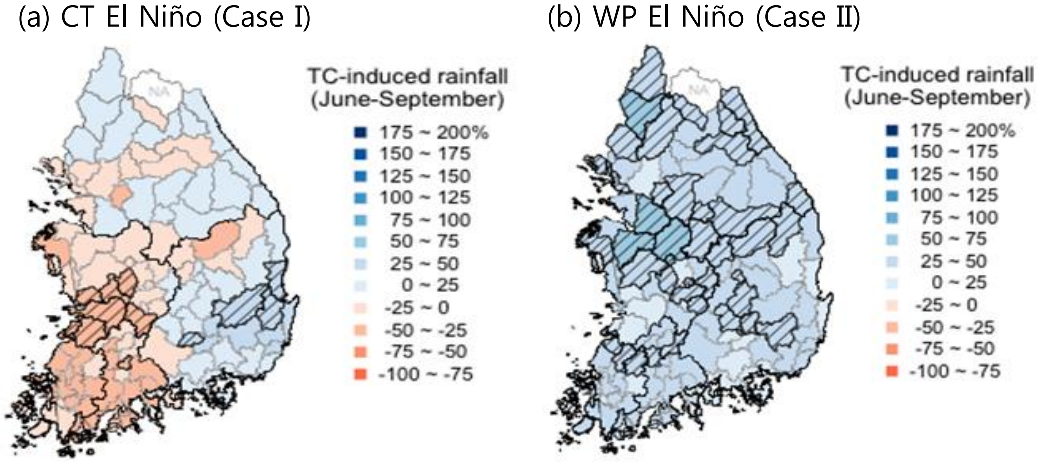

Figure 10. Composite anomalies of TC-related heavy rain days (≥50mm/day) during CT/WP El Niño years. The hatched polygons indicate statistically significant changes in TC-induced rainy days based on the 10% significance level.

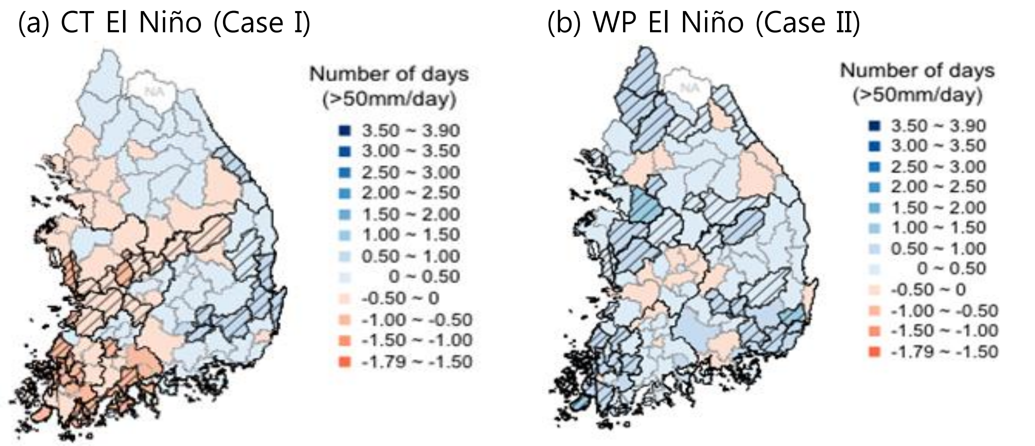

(II-3) Integrated Flood Risk Analysis in the Korean Han River Basin

Integrated Flood Risk Map for Decision Making

Conceptual Framework

- Development of a hierarchy for flood risk index incorporating several factors
  - Categorized: Hydrological, Socio-economic, and Ecological criteria
  - ENSO, TC, and Extreme rainfall indicators

Risk = Hazard + Vulnerability , (Maskrey, 1989)

Goal	Criteria	Components	Determinants	Indicators
Integrated Risk Index (IRI)	Hazard	Hydrologic	Trigger	Rainfall totals (H_1) Peak rainfall (H_2) Frequency of extreme events (H_3)
			Condition	Elevation (H_4) Slope (H_5) SCS CN (H_6): Land use, Soil type
			Response	Flow volume (H_7) Peak flow (H_8) Flood area (H_9)
	Vulnerability	Socio-Economic	Exposure	Population (S_1) Housing (S_2) Urbanization (S_3) Road (S_4)
			Susceptibility	Farmer production (S_5) Industry production (S_6)
			Resilience	Refuge facility (S_7)
		Ecological	Biodiversity	Forest rate (E_1)
			Pollution loads	BOD pollution load (E_2) TN pollution load (E_3) TP pollution load (E_4)

* *Integrated flood Risk Index (IRI)*
= function (H_i, S_j, E_k)

Hazards Vulnerability

$$IRI(j) = \underbrace{\sum_{i=1}^{l} h_i \times H_{ij}}_{\text{Hazards}} + \underbrace{\sum_{i=1}^{m} s_i \times S_{ij} + \sum_{i=1}^{n} e_i \times E_{ij}}_{\text{Vulnerability}}$$

Han River Basin

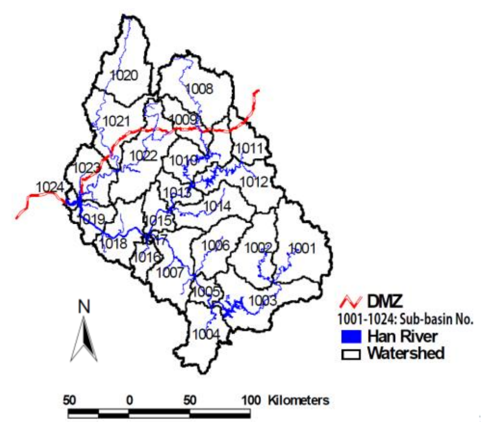

* Data Source: Hydrology data → (WAMIS; http://wamis.go.kr/)
ENSO data → (URL:http://www.cpc.ncep.noaa.gov/data/indices)

Data Collection

Table 1. Hydrologic hazard, socio-economic vulnerability, and ecological vulnerability indices over the Korean Han River basin.

ID	Sub-basin Name	Catchment Area (km^2)	Hydrologic hazard					Socio-economic vulnerability					Ecological vulnerability				
			Annual Precipitation (mm)	Annual Discharge (m^3/s)	Flood Area Density (ha/km^2)	Flood Damage (TW/km^2)	Land Use Urban Area (%)	Population Density (# of person/ km^2)	Housing Density (# of house/ km^2)	Education Density (# of school)	Road Density (Total length/ km^3)	Production (Million Won)	Forest Area (%)	Sewer System (%)	BOD Pollution Load (kg/day)	TN Poiiution Load (kg/day)	TP Pollution Load (kg/day)
1001	Upstream of Namhan River	2447.9	1,240	20,960	0.0425	362	0.5	27.5	12.6	99	457	328,429	84.0	53.0	35,914.6	14,293.4	1,851.2
1002	Phyeongchang River	1773.4	1,294	15,538	0.0274	294	0.6	33.6	14.0	76	441	544,207	82.9	49.0	35,334.4	12,953.9	2,078.6
1003	Chungju Dam	2483.8	1,210	17,504	0.0444	325	1.3	56.4	27.1	130	714	1,506,973	79.8	78.6	66,372.9	24,294.7	3,561.4
1004	Dal Stream	1614.4	1,174	11,410	0.1188	368	2.2	128.4	53.8	137	779	3,622,619	70.8	69.7	117,764.1	42,665.0	8,076.7
1005	Downstream of Chungju Dam	524.4	1,211	3,796	0.1028	702	0.6	47.5	18.1	13	1,101	239,657	64.8	75.0	11,216.3	4,507.1	663.9
1006	Seom River	1491.0	1,298	12,151	0.0441	299	3.6	211.0	71.1	179	780	3,512,228	75.8	59.6	100,118.0	34,146.1	6,458.3
1007	Downstream of Namhan River	2072.7	1,297	16,669	0.2279	288	2.2	190.4	65.6	283	768	13,693,164	49.1	58.4	389,116.2	123,839.8	27,217.4
1008	Kumgangsan Dam	2973.8	NA	NA	NA	NA	NA	NA	NA	NA	NA	NA	NA	NA	NA	NA	NA
1009	Dam of Peace	351.3	1,094	8,263	0.0211	169	0.6	0.6	0.1	1	390	175	91.0	0.0	1,469.1	806.9	75.9
1010	Chuncheon Dam	1587.4	1,187	14,740	0.0069	184	1.2	28.8	10.1	61	431	51,648	84.3	66.5	38,133.5	15,791.6	2,630.0
1011	Inbook Stream	931.3	1,150	8,336	0.0045	283	1.0	15.5	5.7	21	243	19,099	89.6	66.3	9,734.0	4,480.8	531.1
1012	Soyang River	1852.0	1,252	18,975	0.0082	238	0.8	25.0	8.2	37	440	91,659	91.7	69.2	25,795.9	11,264.8	1,414.9
1013	Uiyam Dam	721.7	1,311	7,651	0.0157	104	3.7	340.3	102.3	112	692	370,180	78.6	77.2	74,544.4	26,415.7	4,662.6
1014	Hongcheon River	1566.0	1,303	15,893	0.0112	111	1.3	43.3	15.6	71	434	585,959	86.8	50.3	52,664.3	16,741.8	2,822.4
1015	Cheongphyeong Dam	760.6	1,337	8,019	0.0424	146	1.9	129.5	49.0	61	518	439,297	83.0	54.4	63,126.5	18,520.3	2,885.8
1016	Kyungan Stream	561.1	1,267	5,116	0.0733	154	7.0	275.3	181.5	125	941	8,129,102	64.5	87.9	164,535.9	34,643.6	5,624.9
1017	Paldang Dam	43.9	1,191	395	0.0868	145	1.4	43.8	11.8	10	799	29,773	68.3	60.0	866.8	294.0	31.0
1018	Han River in Seoul	1537.2	1,283	14,681	0.1381	413	31.3	8,070.1	2,107.8	3168	6,428	71,185,977	47.1	93.3	1,256,552.2	288,598.8	31,173.3
1019	Han River in Goyang	826.3	1,260	7,341	0.7535	501	19.7	3,015.2	1,072.0	968	2,998	30,011,536	35.1	69.7	380,297.8	92,935.6	13,600.7
1020	Gomi-tan Stream	2195.2	1,288	20,800	NA	NA	0.3	NA	NA	NA	NA	NA	89.4	NA	NA	NA	NA
1021	Upstream of Imjin River	2072.7	1,291	19,228	0.0162	48	4.0	2.7	0.9	4	67	26,453	68.6	52.4	8,166.6	3,503.6	627.8
1022	Hanthan River	2452.2	1,293	22,919	0.0690	261	5.0	61.7	58.6	252	532	6,750,242	65.6	57.3	291,107.4	86,709.0	17,241.2
1023	Downstream of Imjin River	1419.2	1,302	12,797	0.2300	198	2.9	63.4	22.2	57	322	1,697,206	56.5	60.4	49,754.9	14,994.6	2,751.6
1024	Downstream of Hantan River	146.4	1,294	1,370	0.3314	85	2.1	31.0	10.0	2	285	188,310	22.3	67.4	1,460.4	486.8	84.3

* Data: WAMIS (www.wamis.go.kr), * *NA* represents that data is not available

Hydrologic Time Series Data

Figure 1. Trend analysis of annual precipitation and runoff during different period in the Han River basin, (Period I: 1966-1990, Period II: 1991-2007)

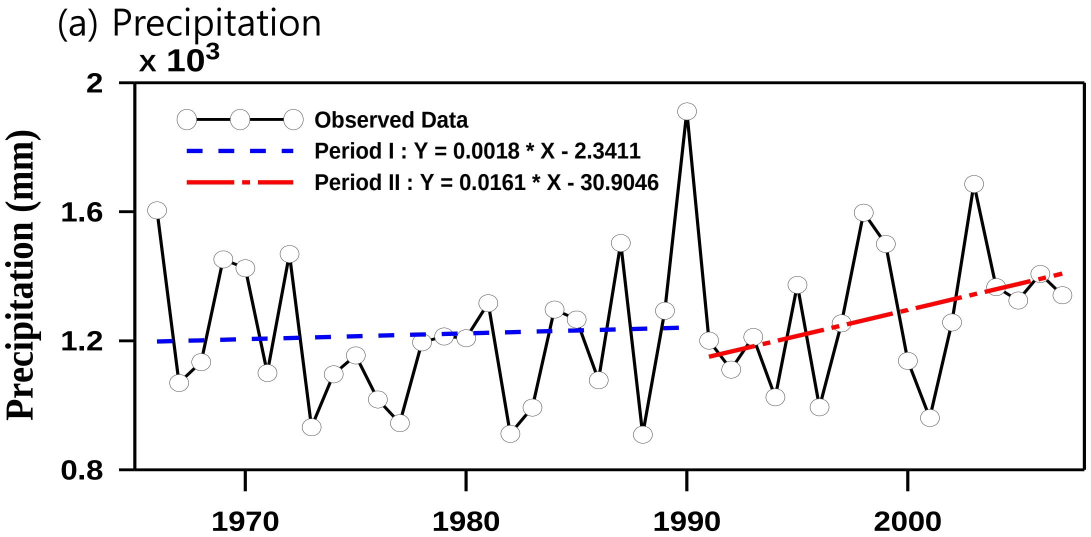

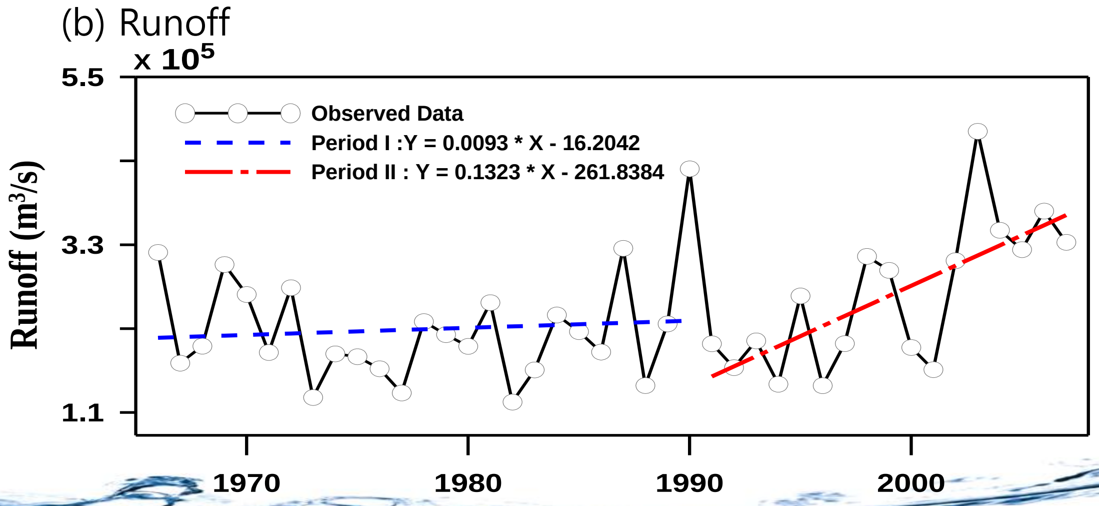

Flood Damage / Flooded Area

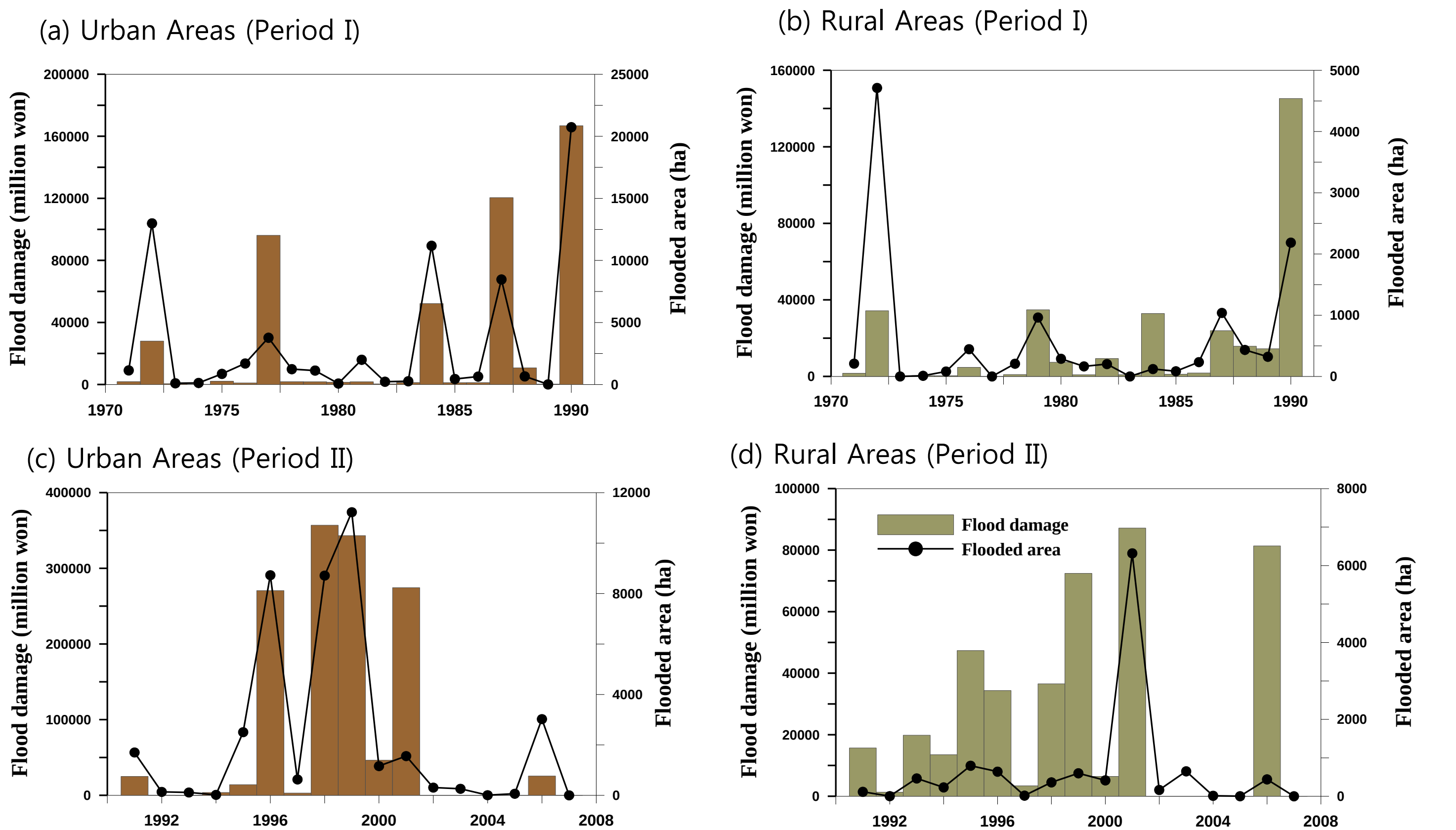

Figure 2. Flood damage and flooded area for urban and rural areas during different periods (Period I: 1971-1990, Period II: 1991-2007).

Ternary Diagrams

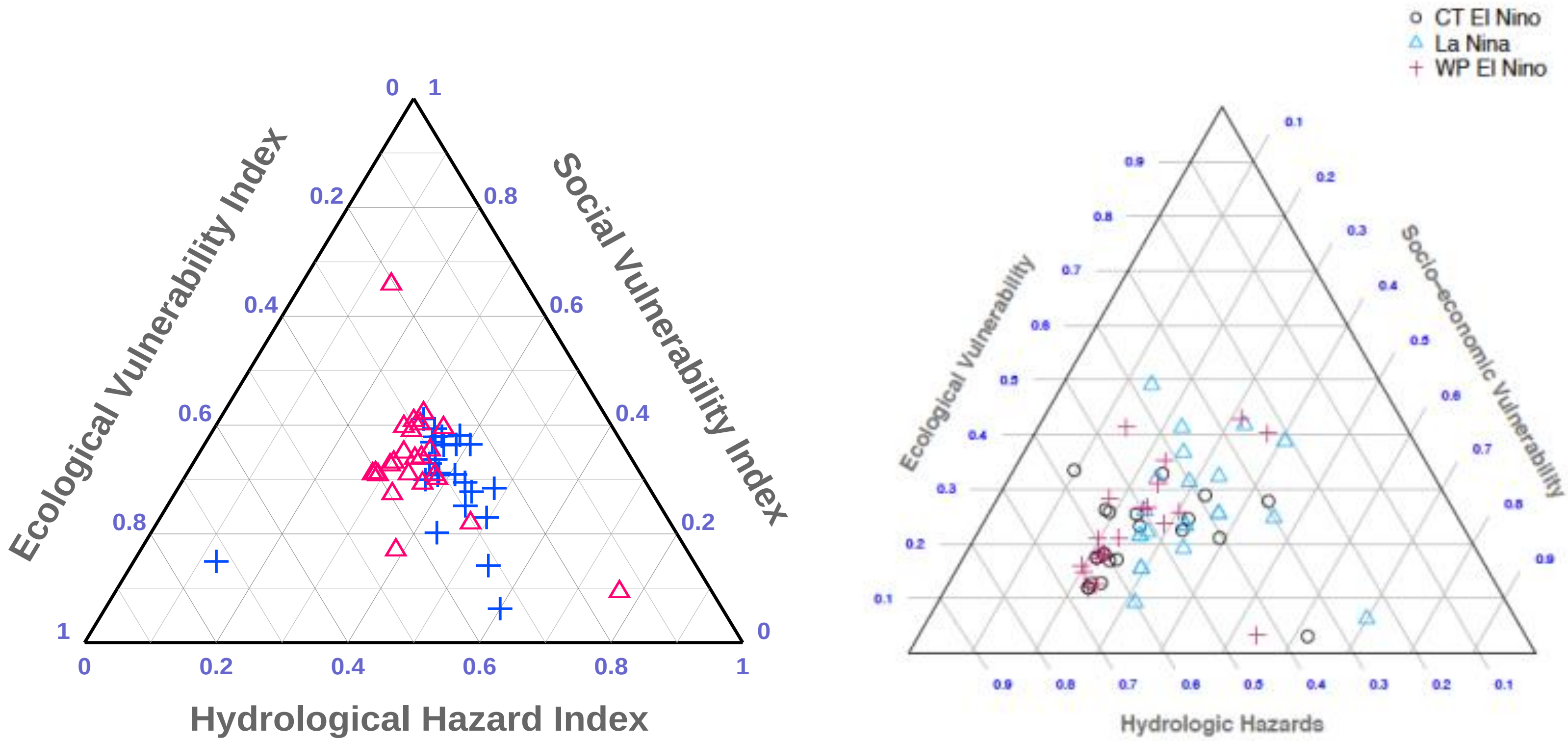

Figure 3. Ternary diagrams for flood risk in the Han River basin between Period I (Red: 1971-1990) and Period II (Blue: 1991-2007), and in different SST conditions. Each point corresponds to fractional indices of flood risk and vulnerability subject to the constraint $H_i + S_j + E_k = 1$..

Radar chart of the Flood Risk Index (FRI)

Figure 4. Radar chart of flood risk index (FRI) between urban areas and rural areas during different periods. (a), (b) show estimated results for FRI on hydrological hazard in urban and rural areas, (c), (d) illustrate estimated results for FRI on socio-economic vulnerability in urban and rural areas, and (e), (f) represent estimated results for FRI on ecological vulnerability in urban and rural areas, respectively. The solid lines indicate FRI for Period I (1971-1990), and the dotted lines indicate FRI for Period II (1991-2007).

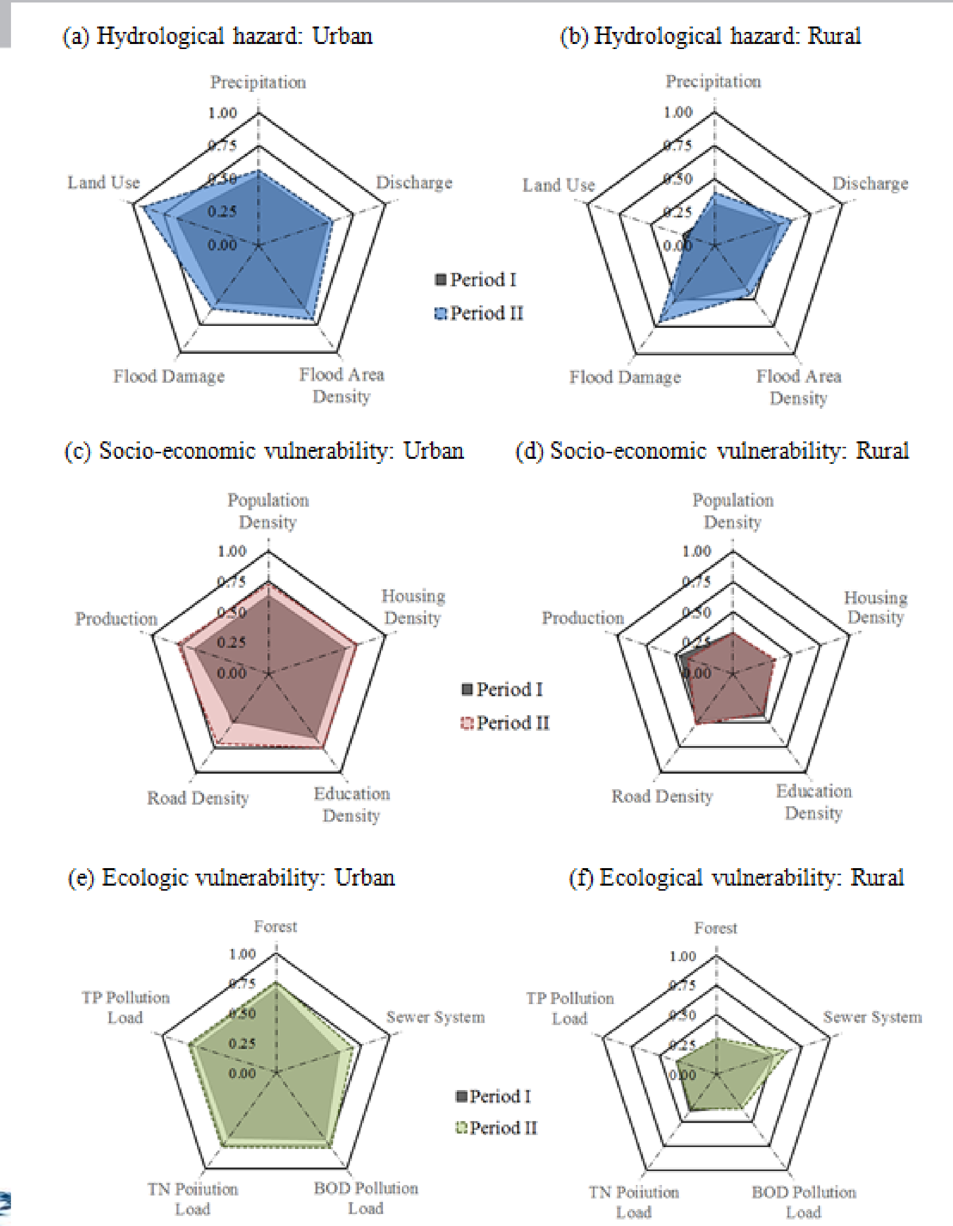

Spatial Distribution of Flood Risk in Different SST conditions

Figure 5. Hydrologic hazard, socio-economic and ecological vulnerability assessment during the different strongest SST conditions over the Han River basin, Korea.

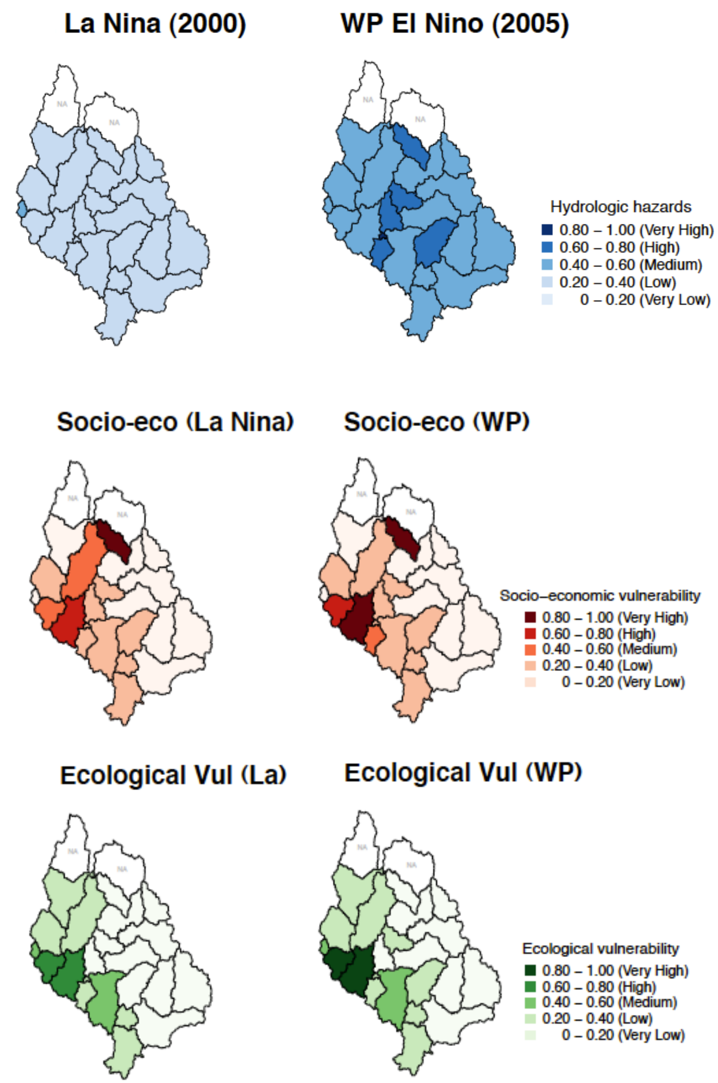

Integrated Flood Risk Map

(1) IFRI in different periods

(a) Flood Risk Index (Period I)　　(b) Flood Risk Index (Period II)

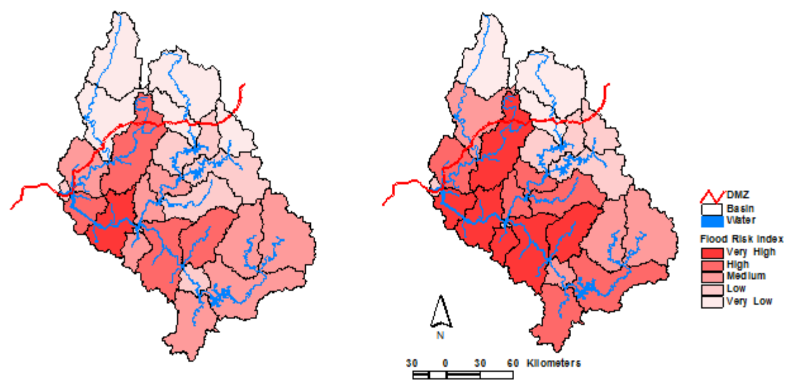

Integrated Flood Risk Index Range	Classification	Coverage (%)		Difference (%)
		Period I	Period II	
1.000 ~ 0.80	Very High	4.47	25.99	21.52 (↑)
0.80 ~ 0.60	High	19.89	24.90	5.01 (↑)
0.60 ~ 0.40	Medium	34.24	19.94	-14.30 (↓)
0.40 ~ 0.20	Low	16.63	13.13	-3.50 (↓)
0.20 ~ 0.00	Very Low	24.78	16.04	-8.74 (↓)

(2) IFRI in extreme SST conditions

La Nina (2000)　　WP El Nino (2005)

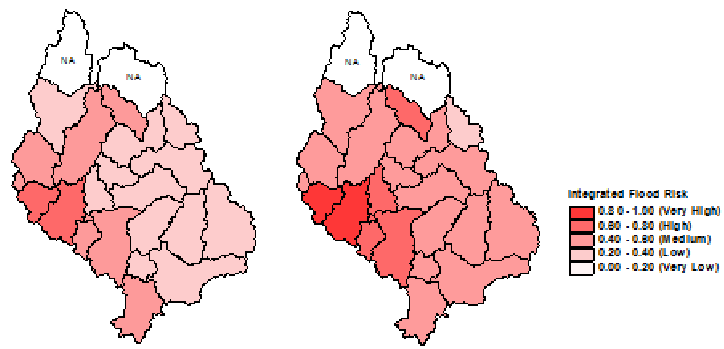

Integrated Flood Risk Index Range	Classification	Coverage (%)	
		La Niña	WP El Niño
1.00 - 0.80	Very High	0.0	8.1
0.80 - 0.60	High	8.1	13.0
0.60 - 0.40	Medium	29.6	75.8
0.40 - 0.20	Low	62.3	3.2
0.20 - 0.00	Very Low	0.0	0.0

III Conclusions

APCC
APEC CLIMATE CENTER

- During WP El Niño years, increased more precipitation and runoff during JJA season better than CT El Niño years over the KP. The findings confirm that water resources in the KP and its sub-basins during the MAM and JJA seasons are sensitive to CT/WP El Niño events.

- The TC-induced summer rainfall over the major Korean river basins decreased from normal years during CT El Niño years (-3.94%) and increased over normal years during WP El Niño years (33.92%).

- The integrated flood risk (IFRI) during WP El Niño year appears increasing tendency than La Niña years. It may provide in developing seasonal hydrologic estimates conditioned upon large-scale climate state for stable water supply and flood risk management in a changing climate.

The findings of relationship between climatic factors and hydrologic parameters are need to support more physical mechanisms in atmospheric sciences. Also it has statistical significance problem due to the lack of data sets. Despite it can be used to sustainable water supply and to the long-range flood forecasting system for water resources management to end-users and stakeholders.

Thank you!

Special Thanks to ..

- ***Dr. Jong-Suk Kim***
- ***Prof. Young-il Moon***
- ***Prof. Shaleen Jain***
- ***Prof. Tae-Sam Lee***
- ***Mr. Sang-Myeong Oh***

SunKwon Yoon, Ph.D.
Climate Change Research Team,
Climate Research Department, APEC Climate Center
Phone: +82-10-9432-3067, Fax: +82-51-745-3999
E-mail: skyoon@apcc21.org

Conceptual Framework for Long-range Flood Forecasting

APCC MME Forecast

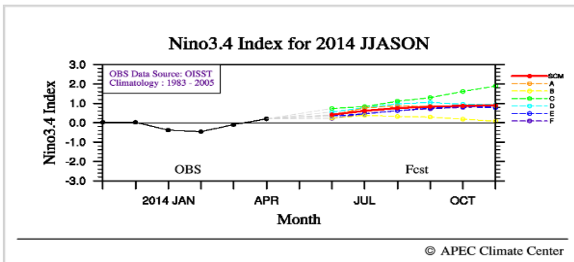

Fig. 1 Predicted Niño 3.4 Index. The predictions from the individual models are marked A, B, C, D, E, and F, while that from the simple composite MME method is marked as SCM.

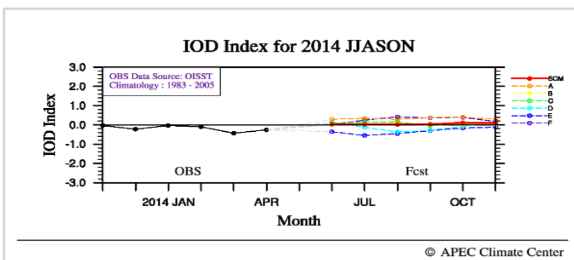

Fig. 2 Same as Fig. 1 but for the Indian Ocean Dipole mode index (IODMI).

Streamflow Forecast

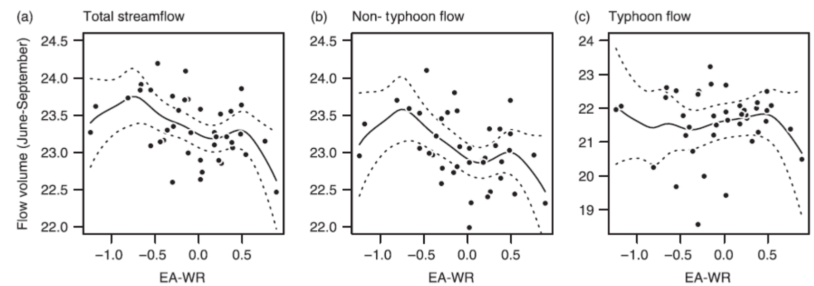

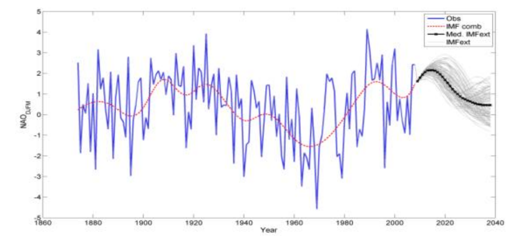

Long-range Flood Risk

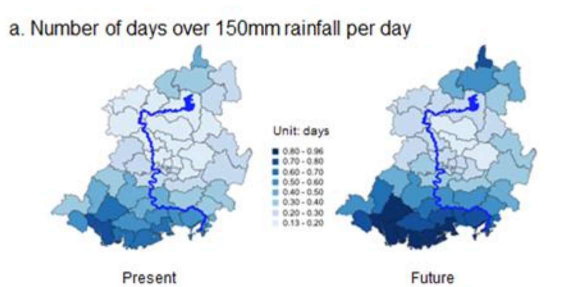

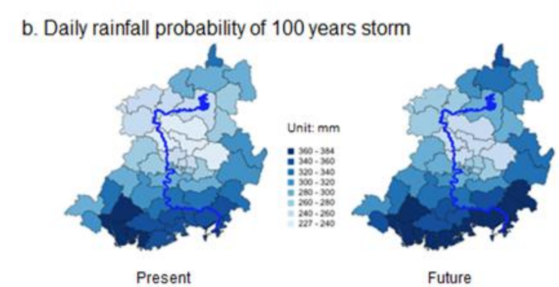

Empirical estimates of typhoon-induced streamflow

→ *4-day time window: 98% of the historical typhoon events with intercepts in the Korean domain*

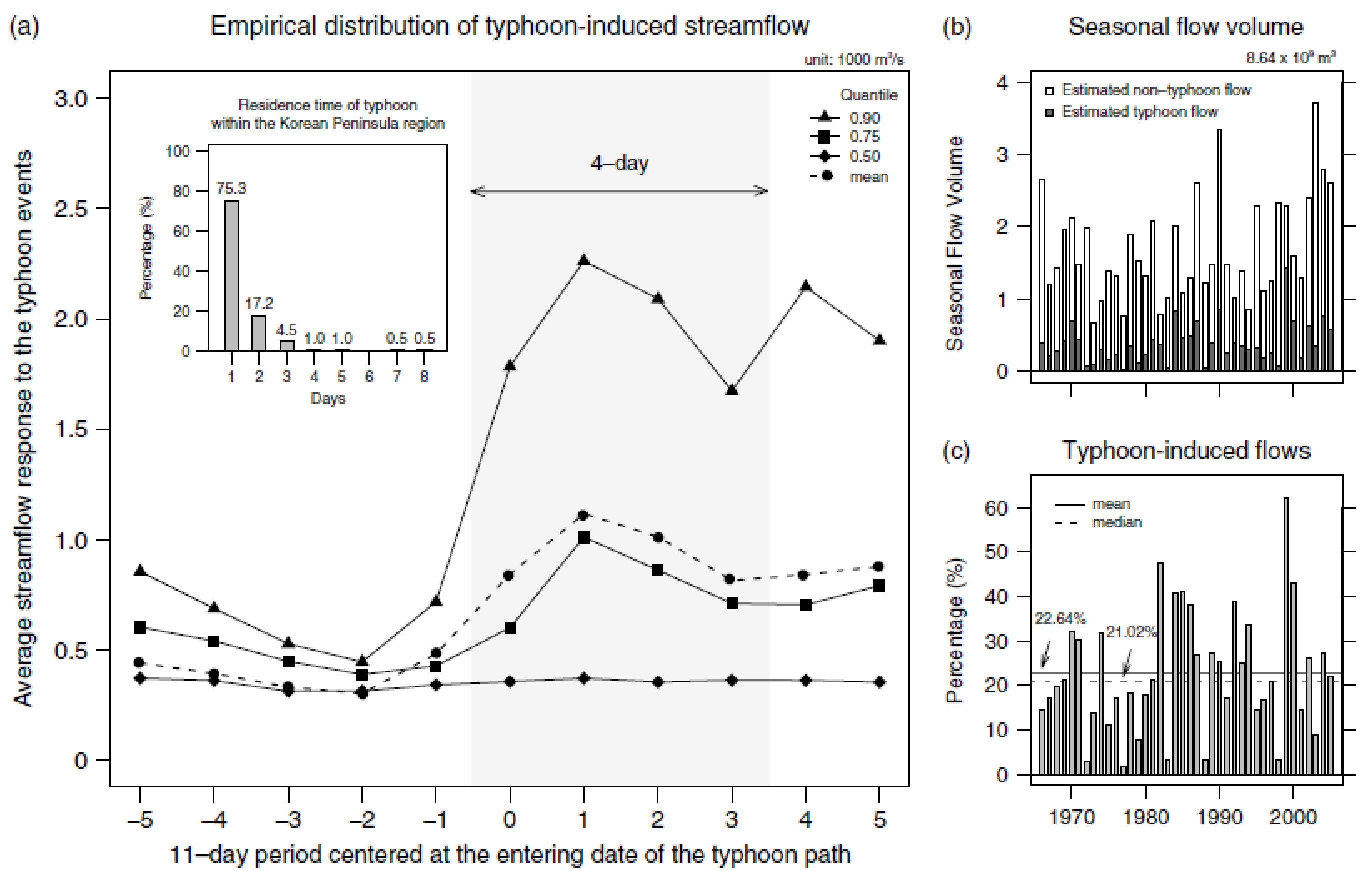

Source: Kim *et al.* 2012, IJOC

Typhoon Tracks and Daily Discharge

Based on the historical record (1966–2005), 198 typhoon storm tracks have been recorded within the restricted Korean domain (120 °E–138 °E, 32°N–40°N)

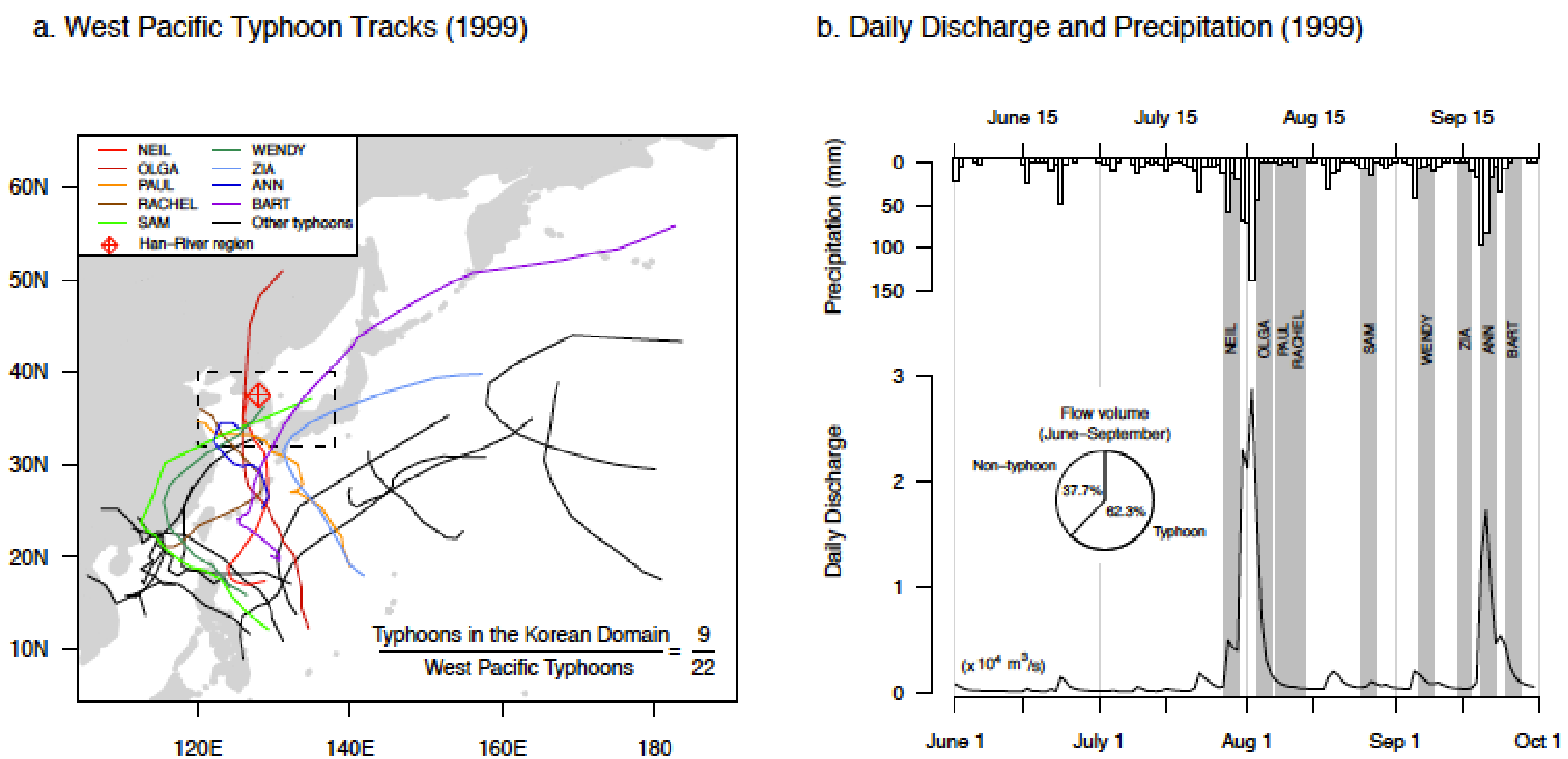

Source: Kim *et al.*